Simulation of Flexural and Tensile Properties of Additively Manufactured Continuous Carbone Fiber

Garshasp Keyvan Sarkon

Submitted to the
Institute of Graduate Studies and Research
in partial fulfillment of the requirements for the degree of

Master of Science
in
Mechanical Engineering

Eastern Mediterranean University
June 2022
Gazimağusa, North Cyprus

Approval of the Institute of Graduate Studies and Research

Prof. Dr. Ali Hakan Ulusoy
Director

I certify that this thesis satisfies all the requirements as a thesis for the degree of Master of Science in Mechanical Engineering.

Assoc. Prof. Dr. Murat Özdenefe
Chair, Department of Mechanical Engineering

We certify that we have read this thesis and that in our opinion it is fully adequate in scope and quality as a thesis for the degree of Master of Science in Mechanical Engineering.

Prof. Dr. Qasim Zeeshan
Co-Supervisor

Asst. Prof. Dr. Babak Safaei
Supervisor

Examining Committee

1. Assoc. Prof. Dr. Shaban Ismael Albrka

2. Asst. Prof. Dr. Mohammed Bsher A. Asmael

3. Asst. Prof. Dr. Babak Safaei

ABSTRACT

The act of additive manufacturing (AM) entails layer by layer creation of a layered structure from the ground up. This competence allows for a sophisticated design to be carried out with geometries that are sometimes impossible to achieve and materialize with conventional manufacturing methods such as subtractive manufacturing, molding, foaming, etc. Fused filament fabrication (FFF) or sometimes addressed as fused deposition modeling (FDM) is among the AM methods which couples well with manufacturing composite materials. Fabricated composite materials using FFF has proven to be particularly useful in a plethora of industries, namely in the aerospace and aeronautics, automotive industry, therapeutic apparatuses, and sports goods. In general, invented parts with FFF method have excellent mechanical properties which make them worthy of further study. Performance under tensile tension and flexural (bending) tensions are particularly significant in composite materials. Therefore, a thorough finite element modeling (FEM) on tensile and flexural behavior of FFF fabricated continuous carbon fiber specimen in the COMSOL multi-physics® environment is executed while using layered shell elements to express the properties in a layered structure. The results gathered from the FEM was compared to other experimental and related empirical studies. Furthermore, the type of effects a composite material might have on tensile properties such as infill ratio, infill pattern, fiber content, layer orientation and stacking sequence will be put under scope. Based on the results provided under this new study, the tensile and flexural simulated specimen shown better maximum tensile and flexural capabilities, with 1490 [MPa] and 1240 [MPa] Max stress, while the tensile model underwent the boundary load of

559.9 MPa and the flexural model went through 302.70 N at two points to simulate the two-point flexure test.

Keywords: Tensile and Flexural Properties, 3D Printing, Fused Filament Fabrication, Finite Element Modeling, Carbon Fiber Composites

ÖZ

Eklemeli imalat (AM) uygulaması, bir numunenin sıfırdan katman katman oluşturulmasını gerektirir. Bu yetenek, diğer geleneksel üretim yöntemleriyle bazen oluşturulması imkansız olan geometrilerle karmaşık bir tasarımın gerçekleştirilmesine olanak tanır. Erimiş filament üretimi (FFF), kompozit malzemelerle iyi eşleşen AM yöntemleri arasındadır. FFF kullanan fabrikasyon kompozit malzemelerin, otomotiv endüstrisi, havacılık, tıbbi cihazlar ve spor ürünleri gibi sayısız endüstride özellikle yararlı olduğu kanıtlanmıştır. Genel olarak, FFF yöntemiyle üretilmiş parçalar, onları daha fazla çalışmaya değer kılan mükemmel mekanik özelliklere sahiptir. Gerilim altındaki davranış ve eğilme gerilimleri kompozit malzemelerde özellikle önemlidir. Bu nedenle, COMSOL çoklu fizik ortamında FFF ile üretilmiş sürekli karbon fiber numunenin çekme ve eğilme davranışı üzerine kapsamlı bir sonlu eleman modellemesi (FEM), katmanlı bir yapıdaki özellikleri ifade etmek için katmanlı kabuk elemanları kullanılırken gerçekleştirilir. FEM'den elde edilen sonuçlar, diğer deneysel ve ilgili ampirik çalışmalarla karşılaştırıldı. Ayrıca, dolgu oranı ve deseni, lif içeriği, katman yönelimi ve istifleme sırası gibi bir kompozit malzemenin çekme özellikleri üzerindeki etkilerinin türü de kapsam altına alınacaktır. Bu yeni çalışma kapsamında sağlanan sonuçlara dayanarak, çekme modeli 559.9 MPa sınır yüküne maruz kalırken, çekme ve eğilme simülasyonu numunesi, 1238 [MPa] ve 1652 [MPa] Maks stres ile daha iyi maksimum çekme ve eğilme yetenekleri gösterdi. eğilme modeli, iki nokta eğilme testini simüle etmek için iki noktada 302,70 N'den geçti.

Anahtar Kelimeler : Çekme ve Eğilme özellikleri, 3D baskı, Fused filament üretimi, Sonlu eleman modellemesi, Piezo-elektrik, Karbon fiber kompozitler

DEDICATION

I hereby would like to express my earnest gratitude and veneration to my lovely family for their selfless attention and kindheartedness for without their intellectual, monetary, and emotional support keeping consistency would have been unimaginable.

ACKNOWLEDGMENT

I would like to immeasurably give my reverence to my supervisor, Assistant Professor Dr. Babak Safaei for he truly is inspirational in both academic prowess and disposition. Moreover, my co-supervisor Professor Dr. Qassim Zeeshan for everything that he taught me.

TABLE OF CONTENTS

LIST OF TABLES

LIST OF FIGURES

LIST OF ABBREVIATIONS

AM	Additive Manufacturing
ASTM	American Society for Testing and Materials
BJ	Binder Jetting
CF	Carbon Fiber
CFR	Carbon Fiber Reinforced
CFRP	Carbon Fiber Reinforced Polymer
DED	Direct Energy Deposition
FDM	Fused Deposition Modelling
FEA	Finite Element Analysis
FEM	Finite Element Modelling
FFF	Fused Filament Fabrication
FOSD	First Order Shear Deformation
FRSCM	Fiber Reinforced Structural Composite Material
g	Gravity
Mid-20th	Middle of Twentieth Century
MITC	Mixed Interpolation of Tonsorial Components
PAN	Polyacrylonitrile
PBF	Powder Bed Fusion
3D	3 Dimensional
2D	2 Dimensional
σ_u	Displacement Increment of Stress

Chapter 1

INTRODUCTION

1.1 Background

The practice of manufacturing has been one of the key components of human development and progress through the ages. Some of the most significant methods consist of metal forming, machining, joining, casting, powder metallurgy, and three-dimensional printing or additive manufacturing (AM) [1]. This manufacturing method is already in high demand in many industries, namely aerospace and medical engineering [2,3]. Moreover, considered to be an integral aspect leading to industry 4.0 [4]. In medical applications, AM has become the most commonly applied manufacturing method in hearing aid gadgets, dental implants and prosthetic bones and cartilages [5]. With the availability and commercialization of this technology, even novice, non-technical household applications have been reported to be functional and practical for either maintenance, or self-customization [6].

The methods used in AM can create objects with sophisticated geometry layer after layer [7–17]. Although there are distinct methods under the class of AM, generally the process steps of each method follow the same stages and each steps from different methods of AM fall under the same category (Figure 1.1) [18]. Owning to the aforesaid capabilities of AM technology, researchers are investigating the usage of different materials with this novel method of manufacturing and the usage of fiber reinforced structural composite materials (FRSCM) are no exception in this trend as they possess

superb mechanical properties, highly constructible to best fit the application's demand and lightweight and already applied in many fields and practices. As a result of that, using the aforesaid material paired with the freedom in design which is provided by AM methods is a promising prospect and due to the novelty and lack of data in this method of manufacturing with FRSCM propelled this thesis to further investigate in making improvements in setting the mechanical parameters via choosing a different layer stacking sequence and layer orientation. Two types of different FRSCM were used. For the reinforcement phase, transverse continuous A4S carbon fibers were used and for the matrix phase, commercially named ONYX material from Mark Forged ® Company which are stated to be chopped polymer carbon fibers.

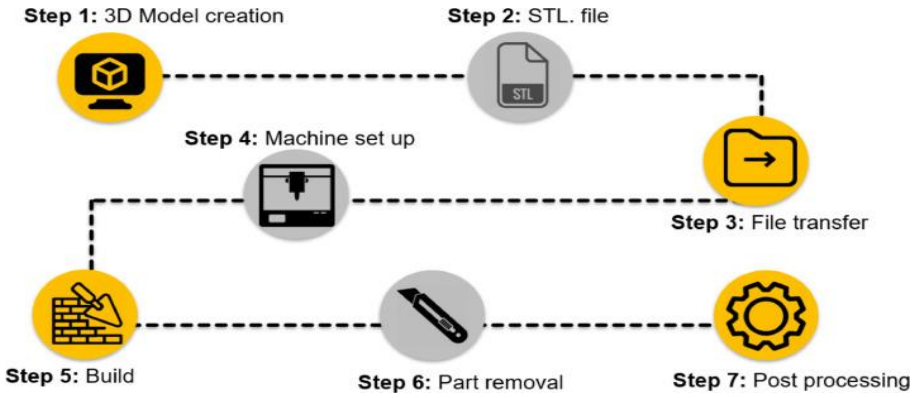

Figure 1.1: The process steps in AM [18]

1.2 Problem Statement

The fact that AM methods are capable of creation of parts with little to no restriction is a great advantage compared to conventional methods[19]. However, the knowledge base for this alternative method of manufacturing is rather limited and in its juvenile state[20]. Therefore, there is much room for further increasing the mechanical properties of additively manufactured parts, namely the flexural (bending) and tensile properties of the printed structures. In this work, it was decided to achieve the aforesaid

goal changing the layer sacking sequence and fiber orientation compared to previous works in order to accomplish better outcomes in terms of more resistance against tensile and flexural stresses. Furthermore, the amount of reliability of a layered material to random and unpredictable orientations of stress is a criterion which will be well-thought-out in layering choice.

1.3 Scope and The Aim of The Thesis

In this work, the main focus of the thesis is improvement in stress bearing capabilities of tensile and flexural carbon fiber reinforced composites manufactured via fused deposition modelling (FFF) technique. This method such as most AM methods is capable of creation of parts layer by layer. Two type of polymer composite materials are used, one known by the name of ONYX material produced by Mark forged®, and AS4 carbon fiber reinforcement layer. The ONYX material is used as matrix material and are implemented as protective layers on the top and bottom of the layered structure, as a result of this setting, the fiber reinforcement layers are stack between ONYX layers on top and bottom. Another aim which is going to be met after the experimental simulation is evaluation of multi-oriented fiber reinforcements. The change in the layering stack of the two different materials and the orientation of the fibers is assumed to improve the behavior of the 3d printed samples and investigation towards this objective is the main goal of this thesis.

1.4 Thesis Contribution

3D printed components, FFF components in particular, are manufactured in way that is unprecedented relative to subtractive and conventional methods due to the fact that the direction of the print dictates the strength of the manufactured part. Owning to that, and the fact that in many applications of printed parts, forces could be applied in

different directions resulting in different oriented stresses within the body following measures are taken to contribute to a more resilient part;

- Solid infill pattern for more density and resistance towards random external forces;
- Multi-oriented reinforcement and matrix phase structure fibers to compensate for the current disadvantage the 3d printed material have;
- Stacking sequence best suited for the specific materials used in the composite structures;
- Overall improved tensile and flexural behavior of the composites compared to previous works.

1.5 Thesis Outline

In the following paper, the first chapter introduces the body of work related to the thesis. Later on, there will be a chapter related to literature review of AM methods, FFF technique and the type of material that is being fabricated which is composite. Moreover, composites will be more under scope and the material used as composites which are carbon fiber reinforced materials. Furthermore, a review on the piezoelectric effect and its fundamental explanation will be included. Thereafter, the mathematical finite element approach that is used for the simulation will be depicted and discussed and finally, the software of choice and the process of simulating will be encompassed within the paper and the final results will be presented, along with a Piezoelectric case study with the use of layer sequencing, orientation, and material.

1.6 Chapter Review

This chapter served as a preliminary introduction to the merit and content of the thesis, presented a general structure and background relating to what was the motivation

behind the research and the details of the inspirational parameters involved in the simulation of the tensile and flexural structures.

Chapter 2

LITERATURE REVIEW

2.1 Introduction to Additive Manufacturing

The most applied AM methods in the industry are FFF or fused deposition modelling (FDM), powder bed fusion (PBF), direct energy deposition (DED), and binder jetting (BJ)[21]. A classification of AM processes is presented (Figure 2.1) [22].

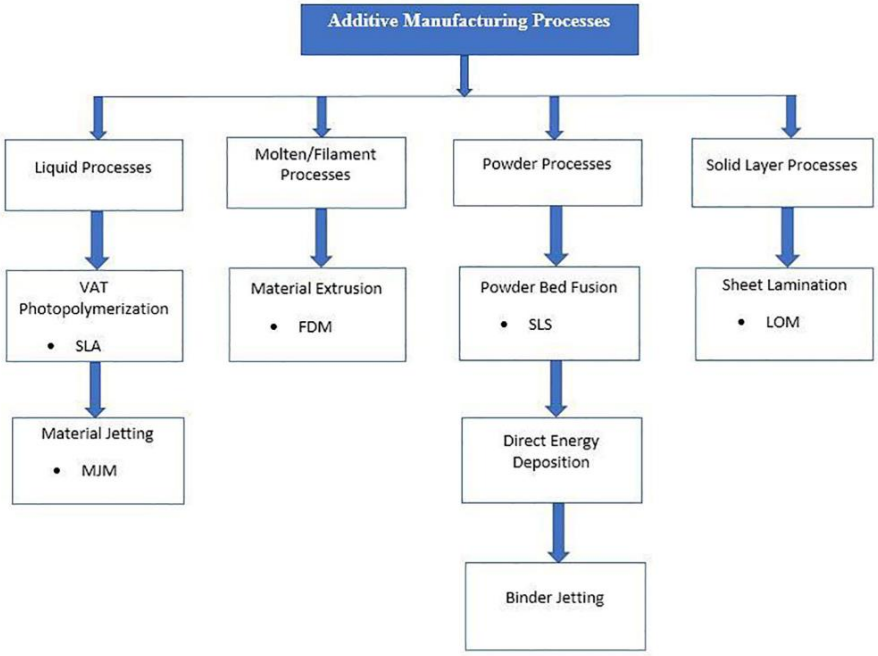

Figure 2.1: Classification of notable methods of AM [22]

Each technique is different in terms of used material, layer formation and printed product. For each material and manufacturing method, different measures and considerations need to be taken to finish the product and to achieve the highest quality. The deliberations and steps required to establish a solid database are distinctive based

on their difference in printing. Therefore, sampling, testing and material analysis in 3D printing methods is based on different criteria. Since each printing method is chosen based on the properties and applications of printed parts, properties differ in terms of surface smoothness, strength, durability, dimension preciseness and geometrical complexity [23]. In this work, the AM method of choice would be FFF due to its low energy requirement, low cost and wide range of applications [24]. Furthermore, it is amongst the AM methods which is capable of using polymer based filaments with chopped, short or continuous carbon fibers either embedded in the filaments or to be added as reinforcements, as pure polymers cannot possess the same mechanical properties as their reinforced counterparts [25] and In this study, it is attempted to simulate a structure manufactured via FFF method with carbon fiber composites with FEM methods. Moreover, it is worth pointing out that the advantages brought about by AM methods which leads to freedom in fabrication of complex geometries opens doors to many possibilities in many applications. As a result, in the field of piezoelectricity and energy harvesting, this possibility is very promising [24]. With constructing the geometry of actuators and piezoelectric structures in geometries never seen before with subtractive and traditional means of manufacturing, piezoelectric output is increased and taking advantage of excellent properties of carbon fibers in piezocomposites can be a significant positive pivotal point for applications of AM in piezoelectric and practical applications instead of using AM as a means to prototyping. Ultimately, with the aid of data driven models extracted from the data gathered from FEM simulation of the multi-layered composite structure, the possibility to further optimizing the parameters that effect the printed composite will be investigated via constructing a neural network regression analysis.

2.2 Fused Filament Fabrication

Fused filament fabrication (FFF) method (Figure2.2) is extensively used for manufacturing geometrically complex objects in a noticeably short time span to suit customer needs [26]. Furthermore, this method is a relatively cheap and low input energy[27]. With control and command over processing parameters due to the enhanced capability of operating machines, this method could be used to great effect in many fields, such as customized biomedical parts which are becoming easier to produce [28]. In FFF, an uninterrupted strand of a thermoplastic polymer is used to 3D print layers of materials [21]. Even though FFF methods have shown competence in production and development, its full-scale use is compromised by limited materials available in the market. nonetheless, weak and anisotropic mechanical properties due to weak interlayer bonding between each subsequent layer is also another factor which dictates the mechanical quality of the printed parts[29]. As a result, it is of utmost importance to adequately fix process parameters in the stage of fabrication [30,31]. For an ideal print quality, it is of paramount importance to set the process parameters in accordance to the technique and the device that is being used as a printing medium, otherwise the mechanical properties of the printed products will be less ideal and below the standard for real applications. some of the shortcomings which need to be addressed are sample detachment while printing or the wrapping phenomenon [32]. There have been numerous attempts in improving the mechanical properties by changing the most influential parameters in a FFF operation. In a work done by Kajimoto et al. [33], To improve the mechanical properties and tensile properties in particular, an automatic carbon fiber reinforced embedding approach, with epoxy resin in the thickness direction was implemented which resulted in a 45% increase of strength in the tensile test loading aftermath. Furthermore , In another recent attempt

to enhance the mechanical properties of FFF parts by Sandhu et al [34], Polylactic acid filaments were chosen and the critical parameters determined to be layer thickness, raster angle and infill pattern. the overall results signified that a cubic infill pattern with layer thickness of 0.16 mm and raster angle of 60 degrees leads to more ideal mechanical properties. Additionally, in another study carried out by C. Gavali [35], it is pointed out that using chopped carbon fiber reinforcements with a 15% weight of carbon fiber reinforcement shows 32% and 22% enhancement in tensile strength and flexural strength. in general, one of the reasons which makes FFF a good method is the ability to investigate the molding defects of FFF of carbon fiber reinforced polymers [36,37]. Based on the recent findings related to the most optimal parameters leading to better tensile and flexural properties of 3D printed specimen, having carbon fiber as reinforcements, the FEM modelling of aforementioned structures will be evaluated. Moreover, mathematical and analytical assumptions in the modeling process will be discussed in the following sections.

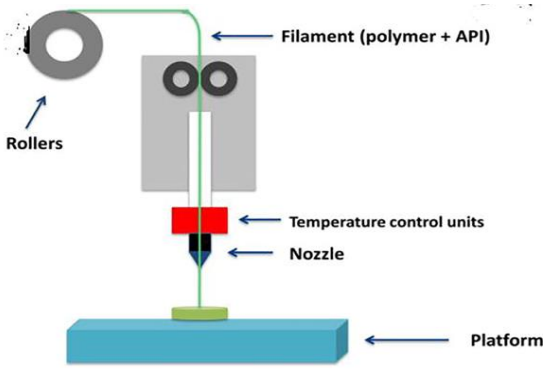

Figure 2.2: A general depiction of a FFF printing process [38]

2.3 Composite Materials

The applications of composite materials go back to well over 6000 years. For the construction of walls, materials such as wattle and daub were used to form a composite wall with preferable mechanical characteristics [39]. They consist of a matrix phase,

reinforcing agent and an intra bounding layer (Figure 2.3). In the recent century however, a composite material with excellent flexural withstanding known as concrete has been of mainstream use. nonetheless, weak tensile capability of concrete is an issue, thus leading to reinforcing the concrete with steel rods to enhance the tensile load bearing ability [40,41]. In general, what adds lots of significance to the composite materials is the fact that these materials are made with customized characteristics unlike conventional materials such as steel or metal and they possess much better physical and mechanical features (Figure 2.4) which fits the intended application of their use. As an example, in aerospace applications, materials that are light in their weight and possess the attributes of metallic materials are highly favorable. As a result of this unique feature in composite materials , their application and manufacturing will be unremitting and highly demanded for the foreseeable and distant future [42,43]. Furthermore, owning to the fact that the simulated composite in this thesis will be of fiber reinforced kind, it is noteworthy to mention that the worldwide demand for fiber reinforced composites is set to grow at a quicker pace since the aerospace industry requires a substantial quantity of the aforesaid CFR material [44]. Also, CFR material are a novel prospect for the biomedical industry which adds even more to their value and demand [43]. Additionally, there are already developing strategies for making the composite material as a sustainable form of material which helps immensely in energy and cost [45]. In conclusion, such great advantages brought about by composite materials paired with the freedom and accuracy of geometry design by AM, makes for an outstanding route and for unprecedented possibilities never fathomed and imagined.

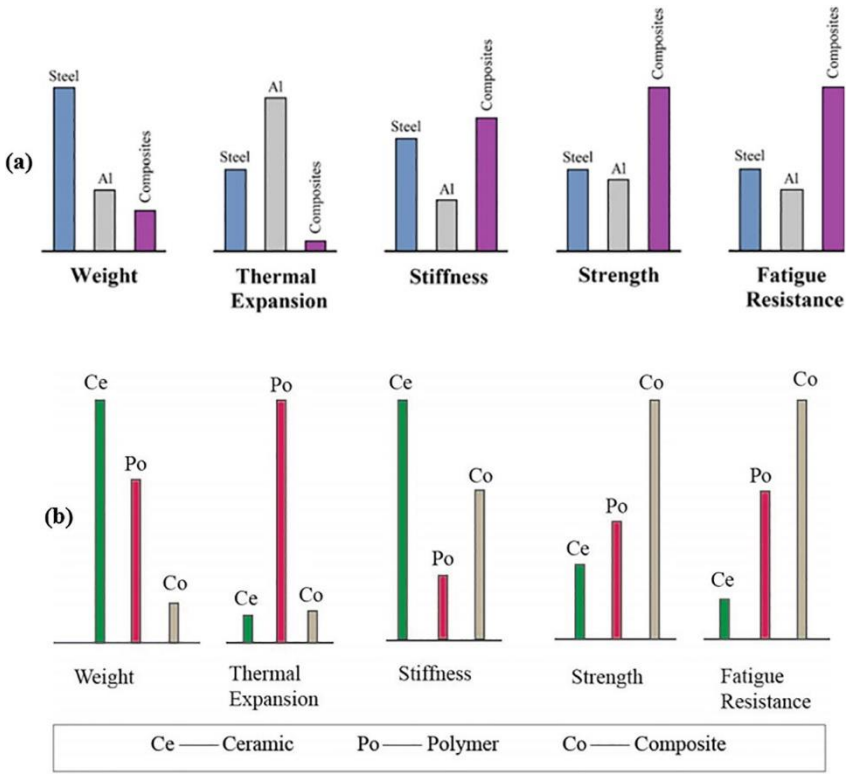

Figure 2.3: **(a),** Comparison of mechanical properties of composites as opposed to pure metallic material. **(b),** Comparison of ceramics and polymers with composite materials [43]

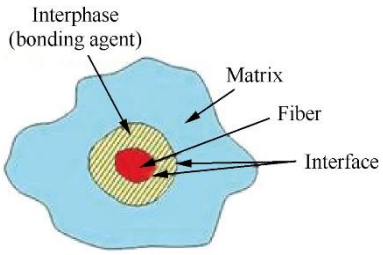

Figure 2.4: General depiction of a matrix, fiber and the bonding phase [46]

2.4 Types of Composite Materials

Owning to the complex nature of composite materials, authors can differentiate and classify them based on many criterions. such as the type of materials that are used as the matrix phase or the reinforcement phase of the composite material Nonetheless, in this paper, composite materials are classified based upon the type of reinforcement that is embedded within them. Based on this consensus, the following Figure (2.5) is considered.

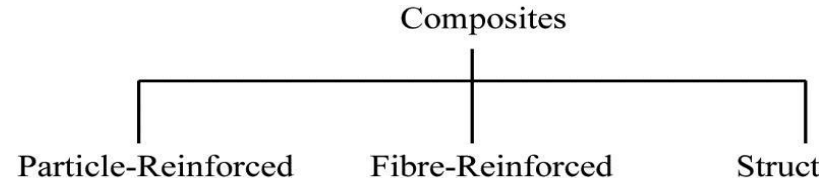

Figure 2.5: Type of classification of composite material based on the reinforcement [43]

In the case of particle – reinforced composites, there are typically two types of particle reinforcements, short particle reinforcers which are based on their proportions could be considered as either dispersion-strengthened composites or large-particle composites. In the case of the latter composite type, the so-called large particles perform as a deformation preventive agent in the areas they exist which is the main reinforcing mechanism that they have. In the case of the former, the nano-sized particles are considered as the reinforcing agent but the difference with the large particle case is the matrix phase typically bears the enforced mechanical load. Due to the small size of the nano-reinforcement agents, the bond which leads to hindering spread of dislocation lines along the matrix phase is via the strengthening the bond on the atomic level [43].

2.5 Rule of Mixture

Estimation of the mechanical values of a given composite material, namely modulus of elasticity, Poisson's ratio, etc. can be forecasted by a method known as the rule of mixture. In this method, each constituent is taken into account with their corresponding mechanical property. Furthermore, the lower and upper bound of a constituent is the range which the mechanical value of composites would typically fall into. Another important parameter in the rule of mixture is the volume fraction of the implemented material. The supposition is that the composite properties is the scaled value of the mean of the constituent's properties on a volumetric basis.

$$E = E_M V_M + E_i V_i (Upper\ bound) \quad (1)$$

$$E = \frac{E_M E_I}{E_M V_I + E_I V_M} \ (Lower\ bound) \quad (2)$$

In the abovementioned equations (1) and (2), the letter E indicates the elasticity and V the volume fraction. Moreover, the letters I and M as subscripts are showing the matrix and in the inclusion phase or in other words, the particulate reinforces. Some crucial parameters which affect the mechanical properties of composite materials are the shape, size, and the spreading of the reinforces, the quality of interface adhesion between the matrix and the inclusions. Overall, the room for deviation in the estimations made via rule of mixture is quite substantial, thus resulting in development of many experimental and theoretical models to make up for the inaccuracies in estimations of mechanical properties of composites [47,48].

2.6 Fiber- Reinforced Composites

The high mechanical properties resulting from implementation of fibrous reinforcements makes them a very good option for improvement of mechanical properties such as modulus of elasticity, strength etc. this method is amongst one of the most implemented choices for improving the composite materials, either for polymer, ceramic or polymer matrix composites. Many factors come in play to determine the overall stiffness and strength of a composite material, such as the properties of each constituent. Additionally, the length to width ratio of fiber, which is a dimensionless criterion, is also very pragmatic. The general consensus is that the minimum length required for a substantial change in the stiffness and strength in a composite is the critical length of a fiber and his quality is directly proportional to the ultimate tensile strength of the material that is used as a fiber and the extent in which the bounding process between the matrix and fiber and the diameter of the fiber itself. The following equation (3) illustrates how critical length is expressed,

$$l_c = \frac{\sigma_f^* d}{2\tau_c} \tag{3}$$

Where l_c indicates the critical length of fiber, σ_f^* is the ultimate tensile strength of fibrous strands and τ_c represents the degree of bonding between fiber and matrix and d is the diameter of the fiber. Due to the complexity of composite material, the tensile and flexural load enforced upon the material could show different behavior depending on the direction of the lead with respect to the direction of the fibers in the material (Figure 2.6). However, this case only applies to continuous and aligned fibers, owning to the fact that dispersed and chopped fibers behave differently. Also, tensile strength of fibers are times stronger compared to the matrix phase. Nonetheless, matrix phase is better upon withstanding more strain before failure and have better ductility. Based on the orientation of fibers and their density and ratio, fiber reinforced materials are classified into three distinct group of continuous – long and aligned, discontinuous short and aligned , and discontinuous and randomly oriented [43,49,50].

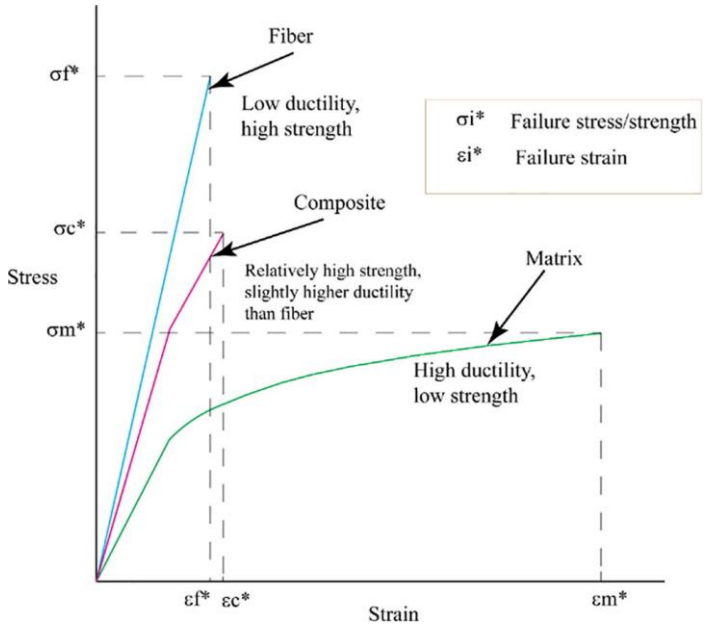

Figure 2.6: Stress–strain graph of a continuous and aligned fiber-reinforced composite while undergoing longitudinal load. Behavior of a brittle fiber and a ductile matrix is depicted as well [43]

2.7 Polymer Carbon Fiber Reinforced Composites and Reinforcements

In carbon fiber reinforced composite materials, where the carbon fiber is implemented for the purpose of enhancing the properties of a given material, the matrix phase could be in a metal, ceramic or a polymer. Carbon fiber reinforced polymer (CFRP) composites are used abundantly in aerospace and aviation [51]. CFRP are renowned owning to their superb high fatigue resistance, low weight, high strength and stiffness [52,53]. These materials are heterogeneous and they do not behave in the same manner as the plastic material do under stress and they are considered to be anisotropic. Furthermore, they have impressive wear, thermal and chemical resistance, namely resistance to oxidation [54].

2.8 Composition of a CFRP

As the name might indicate, CFRP are consist of carbon fibers placed within a polymer resin agent and the carbon fibers work as reinforcements and matrix is the epoxy resin [55]. Figure 2.7 shows a structure of the aforesaid characteristics.

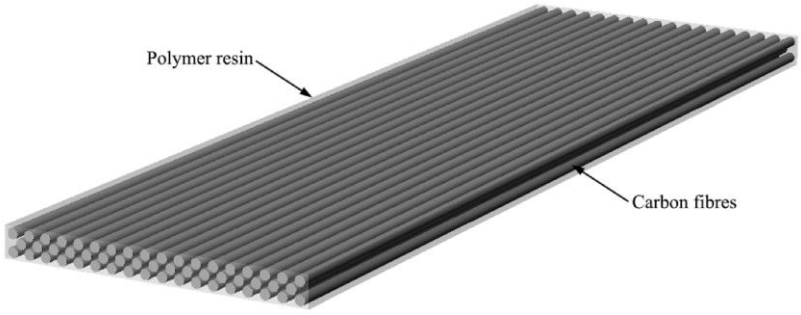

Figure 2.7: A CFRP structure schematic illustration [56]

The general consensus for considering a material as a carbon fiber is at least 90 percent of the weight of the material should be carbon. They often can be derived from polymetric precursor materials, namely cellulose, polyacrylonitrile, pitch and

polyacrylonitrile and the aforementioned materials are processed to become carbon fibers by a number of methods such as heating and tensioning. Carbon fibers are extremely fine materials with the diameter of 5 to 10 μm. The thickness of a strand of carbon fiber is compared to human hair in the Figure 2.8.

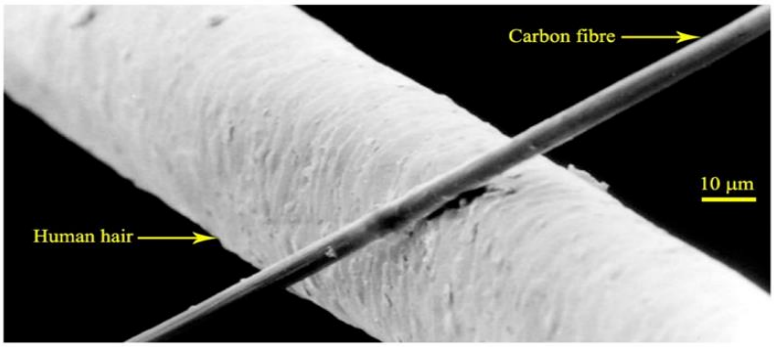

Figure 2.8: Comparison of carbon fiber to human hair [56]

There are records of usage of carbon fibers as early as 1879 by Thomas Edison, which is believed he implemented for light bulbs [57]. Nonetheless, in the mid-20th century, high quality and reliable prototypes of carbon fibers were manufactured [58]. After accumulation of decades of trial and error and insight in manufacturing carbon fibers, remarkable verity of carbon fibers with different properties are available and used in engineering applications. Table 2.1 below shows carbon fibers as significantly better tensile properties compared to presented sample steel materials, while having much lower densities. Moreover, the point in which breakage happens is a good parameter to evaluate to make strength to weight comparisons which is defined as maximum length that a bar of a certain material could hold its own weight. Needless to say that the unit $\sigma_u/(\rho g)$ is the scale of measuring such observation and g is the constant gravity at 9.8 m/s^2 and it is clear that carbon fiber materials have substantial advantage over sample steel material [56].

Table 2.1: Mechanical properties of carbon fiber as opposed to steel sample materials [56]

Type	Name	Density ρ (kg/m^3)	Tensile Strength σ_u (GPa)	Elastic Modulus E (GPa)	Breaking Length $\sigma_u/(\rho g)$ (km)
Carbon fiber	Standard	1760	3.53	230	205
	High strength	1820	7.06	294	396
	High modulus	1870	3.45	441	188
Steel	S355	7850	0.50	210	6
	wire	7850	1.77	210	23

2.9 Structural Composites

The name structural composite refers to the type of material that are formed upon careful stacking of composite laminates via an adhesive agent. Typically, the mechanical behavior of the stacked laminates which form the composite structure is dependent upon a number of criteria, namely the constituent's properties, the size, shape and dimensions of the structure in bulk mode. There are mostly two distinctive type of structural composites, sandwich structures and laminated structures. The laminate structures (Figure 2.9) are the type of structure that is printed in a FFF process so therefore the focus is more gravitated towards this type of material. Basically, they are made of 2 dimensional plies which are set on top of one another and could be oriented to any direction depending on the application and the predicted direction of load in application. sheets are typically continuous and aligned fibrous composites. Furthermore, the idea behind addressing the plies as 2 dimensional is merely due to

the fact that the length to thickness ratio is drastically high in favor of the length[59]. Owning to this feature, the idea behind FFF process is that each ply that is printed is considered to be a 2-dimensional ply, with the same analogy as laminated structural composites.

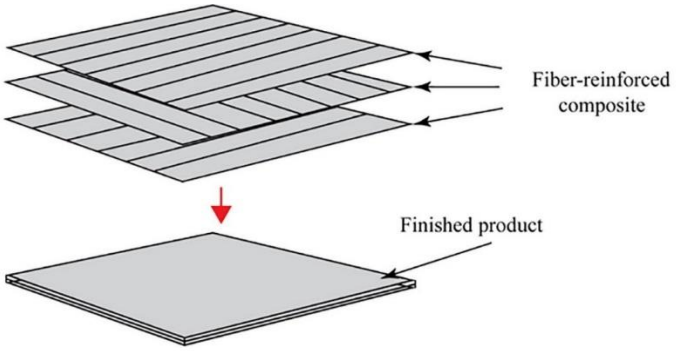

Figure 2.9: An example of a laminated composite structure [43]

2.10 Chapter Review

In the previous chapter, a review of the purpose and ideology behind AM and in particular FFF method of fabricating 3D objects were reviewed. The material of choice which is a composite material was reviewed, type of composites which were of carbon fiber reinforced was determined and put under scope and the rule for determining the material related parameters to be set for composites, known as the rule of mixture was explained. Moreover, depending on the type of application, the structural composites were designated for explanation which is the type of application in the simulation of the thesis.

Chapter 3

MODELLING FINITE ELEMENT ANALYSIS IN COMSOL MULTIPHYSICS

3.1 Research Methodology

The research that is set to be carried out is of a FEA simulation approach. As a result of that, parameters of interest which are fiber orientation (angle), sequencing and number of layers. All parameters are held identical to research done by Ghebretinsae et al. [60], while the aforementioned parameters of interest are changed based on study by Parmiggiani et al. [61] to evaluate their significance in the aftermath of the study. Furthermore, for the sake of similarity, in the ongoing study, fiber volume fraction is assumed to be 35% while the other 65% is considered to be polymer resin and epoxies to consider their effect in the structure. Furthermore, in the study by Parmiggiani et al. [61], the fiber volume is set to be above 50%.

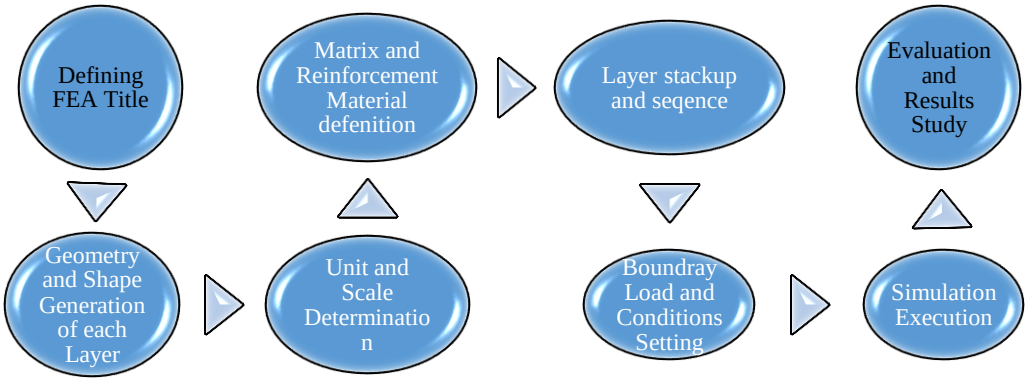

Figure 3.1: Flowchart of the steps in simulation modeling

3.2 COMSOL Multiphysics

COMSOL Multiphysics is a general purpose finite element analysis (FEA) software which has the option of incorporating different physics interfaces in a given modelling environment convenient for either user defined or built-in choices depending on the modelling task at hand [62]. Furthermore, COMSOL Multiphysics features numerous central variables and functions (e.g., domain and path incorporation options) which is very helpful tool in following the workflow of the process of modelling. Moreover, because of the multiple live links that could be established to other application, such as excel, MATLAB etc. which would be very helpful in further investigating the applications of the simulated structure in future works [63]. in COMSOL environment, for simulating a 3d printed structure, the structural mechanics node is used, and the layered shell interface is further selected which allows for modelling composite materials. In general, because of the layer wise nature of the FFF process, each fabricated part is regarded and modeled as a composite material. In the following section, more details regarding layered shell interface and how it operates.

3.3 Modeling Composite Materials in COMSOL Multiphysics

Composite materials are essentially important for their remarkable strength and relatively less weight compared to conventional materials. They are inhomogeneous materials having two or more constituents and have a wide variety of applications. One of the most defining aspects of studying composite materials is the scale of analysis. Typically, the analysis could be done on a micro scale (fiber-matrix modeling)[64] or macro scale (Laminate modeling)[65]. difference between these two perspectives is, in the former, calculation of the homogenized material properties of laminas by means of the archetypal unit cell having matrix and fiber materials is recognized as micromechanics analysis. On the other hand, concerning the latter, when dealing with

a composite laminate and considering its response towards different loading conditions, the resulting scope of analysis is known to be a micromechanics analysis[66]. In this simulation study, composites are considered to be orthotropic materials. Homogeneous materials are isotropic, meaning that they could be defined only with Poisson's ratio and young's modulus in a single x-direction. Orthotropic materials on the other hand, need to have nine elastic constants to express the stress-strain reactions of the Hook's law. The Matrix [D]-1 contains the characteristics of the orthotropic material.

Typically, there are orthotropic, anisotropic and isotropic materials and in the following mathematic expressions, isotropic and orthotropic materials are under scope. Orthotropic materials could be explained in three Poisson's ratio expressions, young's modulus and shear modulus respectively, which adds up to nine values [37]. Moreover, isotropic materials are defined with a minimum of two material properties in the direction of the X-axis. The nine aforementioned values which explain the conditions of orthotropic martials are kept in the [D]-1, in equation 4,

$$\{\varepsilon\} = [D^{-1}]\{\varepsilon\} = \begin{bmatrix} \frac{1}{E_x} & \frac{-\nu_{xy}}{E_y} & \frac{-\nu_{zx}}{E_z} & 0 & 0 & 0 \\ \frac{-\nu_{xy}}{E_y} & \frac{1}{E_y} & \frac{-\nu_{zy}}{E_y} & 0 & 0 & 0 \\ \frac{-\nu_{zx}}{E_z} & \frac{-\nu_{yz}}{E_y} & \frac{1}{E_z} & 0 & 0 & 0 \\ 0 & 0 & 0 & \frac{1}{G_{yz}} & 0 & 0 \\ 0 & 0 & 0 & 0 & \frac{1}{G_{zx}} & 0 \\ 0 & 0 & 0 & 0 & 0 & \frac{1}{G_{xy}} \end{bmatrix} \begin{Bmatrix} \sigma_x \\ \sigma_y \\ \sigma_z \\ \sigma_{xy} \\ \sigma_{yz} \\ \sigma_{yx} \end{Bmatrix} \quad (4)$$

In static examination of a simple composite beam under loading condition, the stress generated from the loading burden deflects the beam and as a result of that, the amount of deflection can be found via differentiation and the thin beam theory is applied and the theory is under the assumption that even after deformation, the middle surface stays at a normal orientation. Also, should shear and rotation be disregarded. The related expression will be expressed as noted at equation (21).

In the following analysis, the study of flexural and tensile properties of the FFF modeled composites will be in the micromechanics level and for the purpose of modeling a composite laminate. The considerations made for modeling composite materials are more complex compared to ordinary isotropic materials owning to distinguished response of each layer in the structure. such as layer thickness, material, geometry and orientation with respect to the reference plane (Figure 3.1).

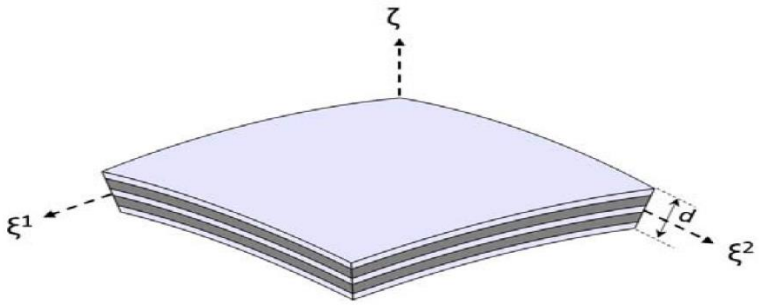

Figure 3.2: An illustration of a three dimensional laminate, with layer stacking and orientation [66]

After determining the scale of analysis, the next step is the selection of the most suitable laminate theory for the task at hand. In COMSOL Multiphysics, two separate laminate theories are implemented. The main theories are first order shear deformation theory and the other is known as 3D elasticity theory. Each theory has its own

advantages which will be illustrated in the following section [66]. Composite laminated structures are formed from laminates which could have different fiber orientation or even different materials in each laminate. Generally, their planar dimensions are two orders of magnitude greater than their thickness. Often laminated structures are implemented in applications necessitating high membrane and bending strengths. So, in many cases composite laminates can be modeled using a shell element based on the equivalent single layer modeling concept. This is a classical way of modeling composite laminates. This theory treats a heterogeneous laminated composite as a statically equivalent single layer. This theory reduces a 3D continuum problem to an equivalent 2D problem, thus reducing the size and computational time of the problem. In addition to simplicity and low computational cost, this theory provides sufficiently accurate description of the global response for a thin to moderately thick laminates such as gross deflections, critical buckling loads, and eigenfrequencies with corresponding mode shapes. In the first order shear deformation theory, In COMSOL Multiphysics, first order shear deformation (ESL-FSDT) theory is one of the options for analyzing composite laminates. This theory is implemented in the Layered Linear Elastic Material model in Shell interface. It has an MITC (mixed interpolation of tensorial components) formulation. As this theory accounts for the transverse shear deformation, it can be used for rather thick shells. One of the most defining features of this theory are;

• Degrees of freedom (3 displacements, 3 rotations) are defined only at the midplane or reference plane of the composite laminate[66]. • Suitable for modeling thin to moderately thick laminates;

• Suitable for finding global response of the laminate e.g., gross deflections, eigenfrequencies, critical buckling load etc.;

• Not very computationally expensive, and thus suitable for analysis of laminates having large number of layers;

• Requires shear correction factor for thicker laminates where transverse shear stresses are not negligible [66].

A layer wise (LW) theory for modeling composite laminates is very similar to a traditional 3D elasticity theory, where the degrees of freedom are only the displacement fields defined in the product geometry created by the reference surface and an extra dimension in the thickness direction. There are two approaches depending on the way degrees of freedom are defined:

I. Partial displacement field approach

II. Full displacement field approach.

In the partial displacement field approach, the laminate thickness remains constant, whereas the full displacement field approach allows a change in thickness of the laminate. In COMSOL Multiphysics, a full displacement field approach-based layer wise theory is implemented in Layered Shell interface. The layer wise theory is more accurate than the equivalent single layer theory, but it comes with the cost of having more degrees of freedom. It is significantly more expensive in terms of computer resources. From accuracy point of view, layer wise theory is as accurate as traditional 3D elasticity theory, but it has several benefits over traditional 3D elasticity theory:

• No need to build a 3D geometry with many thin layers;

• Easy to handle layer wise and interfacial data;

• In-plane finite element meshing is independent of the out-of-plane (thickness direction) meshing;

• A separate, either lower or higher, shape function order can be chosen in the thickness direction in order to avoid shear locking or to gain accuracy advantages [66].

Characteristically, the first order shear theory is derived and a part of the known Kirchhoff-love plate theory. In the aforesaid theory, shear deformations going through the thickness is accounted for in average, which was first suggested by Reissner on 1945 [67] and also 4 years earlier by Mindlin [68]. What makes this theory distinct from the classical plate theory is the assumption that the surface normal to the reference surface is not perpendicular to the middle surface as a result of deformation. Thus, both transverse shear strains and stresses are assumed to be constant through the thickness. In this case, we consider variables u_1 and v_1 to be normal to reference surface and are now dependent upon the rotations of that reference surface, which are denoted as $w_{0,x}$ and $w_{0,y}$ respectively. Based on this theory, the kinematics formed are expressed in five directions, u_0, v_0, u_1, v_1, w_0. If we assume u_1 to be equal to expression ψ_x and ψ_y to be equal to v_1, then the kinematics of deformation is stated by,

$$u = u_0 + z\psi_x, v = v_0 + z\psi_y, w = w_0 \tag{5}$$

Furthermore, curvatures in the structure are denoted as

$$\{k\} = \begin{Bmatrix} \psi_{x,x} \\ \psi_{y,y} \\ \psi_{x,y} + \psi_{y,x} \end{Bmatrix} \tag{6}$$

And the resulting transverse shear strains and stresses are,

$$\begin{Bmatrix} \varepsilon_{yz} \\ \varepsilon_{xz} \end{Bmatrix} = \begin{Bmatrix} \psi_y + \psi_{0,x} \\ \psi_x + \psi_{0,y} \end{Bmatrix} \tag{7}$$

$$\begin{Bmatrix} \sigma_{yz} \\ \sigma_{xz} \end{Bmatrix} = \begin{bmatrix} Q_{44} & Q_{45} \\ Q_{45} & Q_{55} \end{bmatrix} \begin{Bmatrix} \varepsilon_{yz} \\ \varepsilon_{xz} \end{Bmatrix} \tag{8}$$

Now, if we consider the transverse shear forces and strain displacement relationships from integration of equations of motion from 3D elastic material, we get,

$$\sigma_{xx,x} + \sigma_{yx,y} + \sigma_{zx,z} = \rho u_{,tt} \quad (9)$$

$$\sigma_{xy,x} + \sigma_{yy,y} + \sigma_{zy,z} = \rho v_{,tt}\,, \quad (10)$$

$$\sigma_{xz,x} + \sigma_{yz,y} + \sigma_{zz,z} = \rho w_{,tt} \quad (11)$$

With integration of the first two equations (10), (11) in thickness direction, we get two new expressions s following:

$$Nx = \int_{-h/2}^{h/2} \sigma_{xx} dz, \quad (12)$$

$$Ny = \int_{h/2}^{h/2} \sigma_{yy} dz, \quad (13)$$

$$Nxy = \int_{h/2}^{h/2} \sigma_{xy}\, dz, \quad (14)$$

and by adding the in-plan resultant forces,

$$N_{x,x} + N_{xy,y} + q_x = \int_{h/2}^{h/2} \rho u_{,tt} dz \quad (15)$$

$$N_{xy,x} + N_{y.y} + q_y = \int_{h/2}^{h/2} \rho v_{,tt} dz \quad (16)$$

Where q_x and q_y are forces per unit area subsequent from loads applied to the top and bottom surfaces or body forces enforced on the **x** and **y** directions and **h** is the thickness of a laminate. By making an integration through the thickness direction, we attain the transverse shear forces as such,

$$Q_x = \int_{h/2}^{h/2} \sigma_{xz} dz, \quad (17)$$

$$Q_{y = \int_{h/2}^{h/2} \sigma_{yz} dz,} \quad (18)$$

Therefore, the transverse motion is expressed as following,

$$Q_{x,x} + Q_{y.y} + q_z = \int_{h/2}^{h/2} \rho w_{.tt} dz \quad (19)$$

Using the definition of transverse shear forces by referring to equations regarding strain and displacement, the resulting integration yields,

$$\begin{Bmatrix} Q_y \\ Q_x \end{Bmatrix} = k \begin{bmatrix} A_{44} & A_{45} \\ A_{45} & A_{55} \end{bmatrix} \begin{Bmatrix} \psi_Y + W_{0.Y} \\ \psi_X + W_{0.X} \end{Bmatrix} \quad (20)$$

where **k** is an abstract constant which expresses the shear correction factor. This factor is considered due to assumed field displacement resulting in a constant shear strain state. Generally, in a laminated plate structure, the shear stress possess a hyperbolic response which is why the factor **k** is included for the correction of this divergence[69]. In conclusion, given the parameters and the nature of the structure, Equivalent single layer theory was chosen to perform the FEM simulation. With differentiation techniques, the amount of stress and bending effect could be derived. In the assumption made in the single layer beam theory, the surface that is normal-to the beam mid surface remains unchanged after deflection inducing stress is enforced. Moreover, if the shear forces and rotational forces are neglected, then the curvature and strain equation could be expressed as follows,

$$\varepsilon_0 = \frac{\partial_u}{\partial_x}, \quad k=-\frac{\delta^2 w}{\delta x^2}, \quad (21)$$

In the equations above, the symbols ε, κ indicate the strain and curvature respectively. And, u, w shows the quantity of displacement in the x and z direction. Furthermore, normal strain is indicated as,

$$\varepsilon = \varepsilon_0 + zk \quad (22)$$

The reaction moments in the support areas of the structure and the z direction forces while tensile and flexural stress is applied upon the structure is also considered as following,

$$\begin{bmatrix} N \\ M \end{bmatrix} = \begin{bmatrix} A & B \\ B & D \end{bmatrix} \begin{bmatrix} \varepsilon^{\circ} \\ k \end{bmatrix} \quad (23)$$

The matrix A is a mnemonic for the in-plane stiffness and the B matrix the effect of coupling which ascends between the flexure and the membrane action. Moreover, in a scenario where a laminate is symmetric, the B matrix is going to be considered as zero. Plus, the matrix D illustrates the bending stiffness. Moreover, the quantity of strain in the mid-plane, in-plane loads, moment and curvature are shown by the letters ε, N, M, and κ respectively [36].

Furthermore, the axial direction stress is articulated as [69],

$$\sigma x = Q11(\varepsilon_0 + zk) \quad (24)$$

3.4 Modelling Assumptions and Considerations

The material modeled in this simulation are in plane long carbon fiber reinforcements with a polymer based chopped carbon fiber composite known as the commercial name of ONYX composite which is the matrix phase of the tensile modeled structure. ONYX is made from micro-scaled chopped carbon fibers in combination with immensely dense nylon. ONYX material has the advantage of typical toughness of nylon materials added with capable stiffness capacity of carbon fibers [70]. the aforesaid materials are known for smooth surfaces which does not typically require post-processing. their mechanical properties are shown as illustrated in Table 3.1 below [71].

Based on the results extracted from the work done by Bárnik et.al [72], It's better to stack the layers at even numbers as odd numbers lead to structures failing more often and it is recommended to use even numbered layers for 3D printing applications. furthermore, it was determined that samples with higher infill density yielded better tensile properties and solid infill pattern is the most reliable option in scenarios where stresses could be enforced from different and random directions[60,72,73]. As a result,

in an attempt to realize the effects of fiber orientation of carbon fiber reinforced materials made by Parmiggiani et.al [61], the stacking sequence and orientation with the most versatility is selected, where the stacking sequence for tensile model has 8 ONYX layers, 4 on the top, 4 on the bottom with 16 carbon fiber layers in between and same number of and stacking of ONYX material for Flexural model, only difference being the number of carbon fiber layers, which is 24 layers in between. Full details of structures are depicted in Table 3.2.

Table 3.1: Mechanical properties of ONYX material [71]

Young's modulus [GPa]	**Yield stress [MPa]**	**Ultimate stress [MPa]**	**Flexural strength [MPa]**	**Flexural modulus [MPa]**	**Density [g/cm^3]**
1.4	36	30	81	2.9	1.2

Table 3.2: Mechanical and geometrical specifications of simulating samples [61]

Testing method	**Referencing standard**	**Structure Dimensions**	**Fiber**	**Fiber orientation**	**ONYX layers**	**Carbon fiber layers**
Flexural Test	ASTM D 3039	$153.6x14x4$	ONYX	$[0,90,+45,-4$	8	24
Tensile Test	ASTM D 7264	$157.6x16x3$	Carbon fiber	$[0,+45,90,-4$	8	16

Samples were represented as thin layered laminas. because the layers were manufactured in the printing device were made of two types of materials exclusively

the reinforming fiber which is A4S carbon fiber and the matrix phase which was the ONYX material and there is only one type of material contained in each layer. Furthermore, the following assumptions were also prevalent in the FEM process:

1. Linear elasticity in constituent's performance

2. The Onyx material or the matrix, possessing isotropic physical properties.

3. Fibers transversely isotropic in the reinforcement phase

4. Flawless fiber-matrix attachment

5. Absence of any void or imperfections in the simulated models.

Additionally, the matrix phase (Onyx) was thought to be as an isotropic solid and they were reinforced with carbon fiber layers with the following properties depicted in the Tables 3.3 and 3.4 respectively.

Table 3.3: Properties of defined ONYX material in modelling environment

Property	**Value**	**Unit**
Density	0.12	$\frac{Kg}{m^3}$
Tensile Young's modulus (E_{11},E_{22},E_{33})	{1.4E+9, 7.728E+9, 7.728E+9}	Pa
Flexural Young's modulus (E_{11},E_{22},E_{33})	{2.9E+9, 7.728E+9, 7.728E+9}	
Poisson's ratio V_{12}, V_{13}, V_{23}	{0.104, 0.104, 0.121}	1

Shear modulus G_{11},G_{22},G_{33}	{7.728E+9, 7.728E+9, 2.864E+9}	$\frac{N}{m^2}$

Table 3.4: Properties of defined carbon fiber material in modelling environment

Property	Value	Unit
Density	1790	$\frac{Kg}{m^3}$
Tensile Young's modulus (E_{11},E_{22},E_{33})	{54E+9, 7.616E+9, 7.616E+9}	Pa
Flexural Young's modulus (E_{11},E_{22},E_{33})	{51E+9, 7.616E+9, 7.616E+9}	
Poisson's ratio (V_{12}, V_{13}, V_{23})	{0.104, 0.104, 0.121}	1
Shear modulus (G_{11},G_{22},G_{33})	{7.728E+9, 7.728E+9, 2.864E+9}	$\frac{N}{m^2}$

Furthermore, the thickness of each layer is considered to be 0.125 mm because the thickness of each printed layer is inspired after Mark forged® FFF printing device and each and every layer was presumed as a lamina, while in execution, the bonding quality crammed amongst the adjacent material strand is relatively weaker. Moreover, the ONYX material comprises of chopped carbon fiber pieces. One needs to acknowledge that the type of carbon fiber in a FFF process is not the same material and possess

dissimilar mechanical properties. As an example, the reinforcement carbon fiber modeled and simulated in this study is aimed to have the same properties of Mark Forged® printed carbon fibers. They were recorded to have a bending and tensile elastic modulus of 51 GPa and 54 GPa, correspondingly [74], although a carbon fiber prepared by the method known as PAN manufacturing method bears a tensile elastic modulus of 230 GPa. The finite element models established, were created in similar way with the 3D creation procedures as the test specimen. Yet, the model is set to have no frail bonding amongst the layers which invadable due to current status quo of FFF method. In nature, composite materials are more complex than conventional materials and many considerations need to be taken and because of the orthotropic nature of the material, thus the orthotropic properties in each direction should be defined. In the cases where material is orthotropic, material properties should be defined in x, y, z direction and in the isotropic cases, material specifications should be defined in the x direction only. Subsequently, due to orthotopically of the material defined in the FEA, 3 Poisson's ratio, 3 shear moduli and 3 elastic moduli must be defined. Therefore (v12, v23, v31) for the Poisson's ratio, (G12, G23, G31) for shear and (E1, E2, E3) for elastic expressions, each in three separate orthotropic directions and the subscript numbers along each letter indicates direction where 1,2,3 is set for x, y, z [34]. In a mesoscale analysis of stress and strains, properties of each lamina are needed for procurement of objective quantities in a lamina and the material properties will be defined within the COMSOL environment. A Laminate Stacking Scheme was implemented to generate the 0.125 mm thick laminas and material specifications and their values defined. The lay-up was stacked in similar way as in the FFF setting recommended by Parmiggiani et al. [61] Hence, for the tensile model four layers of ONYX material at the floor and at roof of the samples oriented at [0/+45/90/-45] degrees and 16 unidirectional

reinforcing fibrous layers amongst the roof and floor of the simulated model were provided and Overall 24 lamina of 0.125 mm thickness was joint to make for a 3 mm thick laminate (Figure 3.4 and 3.5). The bending model had 4 layers of floor with Onyx material, then 24 layers of carbon fiber stacked on top of the aforesaid ONYX material, accompanied by 4 layers of ONYX material as the floor layers. 4 layers of roofs were considered in simulation to imitate the protective effect of matrix phase to shield the carbon fiber from damage and furthermore, Total 32 layers of 0,125 mm thickness lamina were used to make a 4 mm thick laminate and the orientation order of comprising layers are [0/90/+45/-45] (Figure 3.6). Additionally, the geometry of tensile and flexural models were in accordance with ASTM D 3039 [75] and ASTM D 7264 respectively [76].

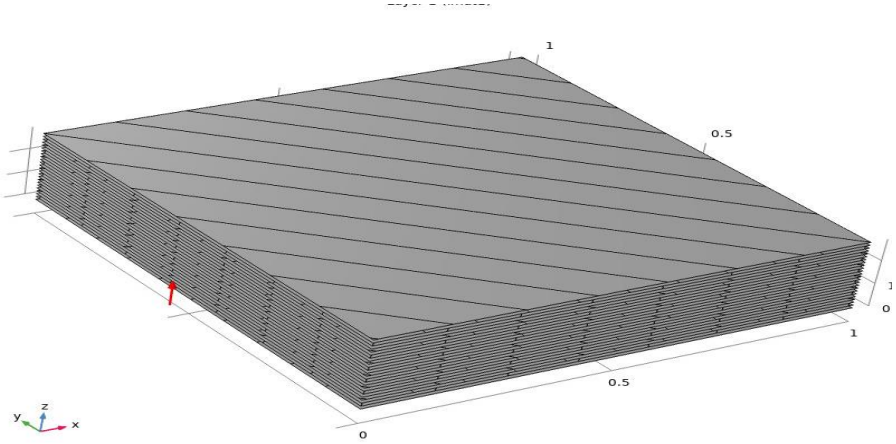

Figure 3.5: A general geometry of the laminate structure

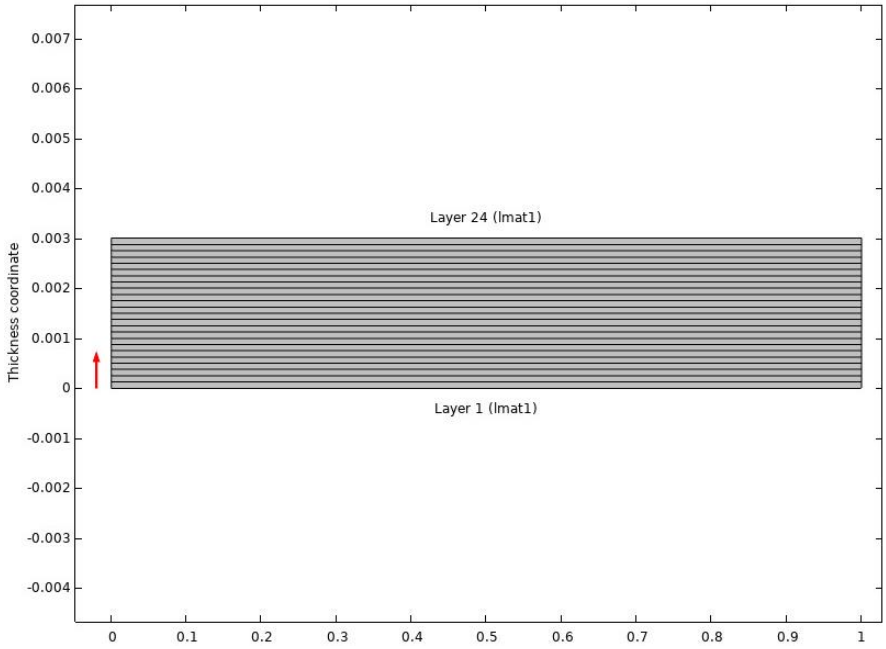

Figure 3.6: Thickness of the tensile animated structure the first layer at the bottom while the last layer (layer number 24) is stacked at the top of the layered material which is equal to 0.003 meters

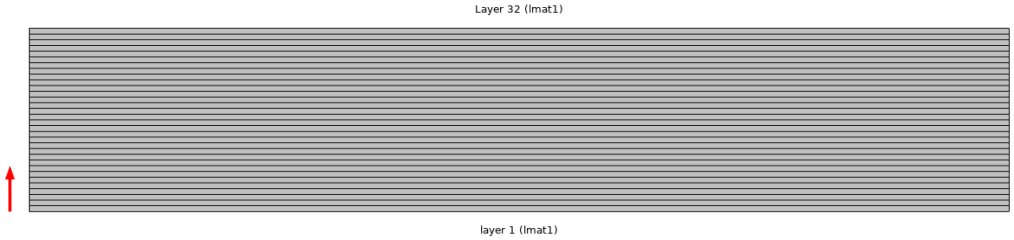

Figure 3.7: Layered display of flexural structure

3.5 Meshing

The meshing process is divided into two general steps, the type of meshing element chosen for segmented FEM analysis, which in the case of this study is chosen to be tetrahedral because of the fact that mesh size is very fine compared to the geometric dimensions of the structure and the second step, which is mesh control. Furthermore, based on the fact that the fabricated material has a composite multilayered nature, based on the type of mesh selection applied in the work done by Matveev et al [77], it

was observed at the boundaries between layers, typical voxelate shaped could result in some inaccuracies and in order to circumvent the issue, tetrahedral shaped elements were chosen. Moreover, owning to rather linear shape of the structure meshes are perceived to be almost evenly distributed among the surface of the multi-layered structure. Furthermore, the specimen consists of 360 mesh vertices. Meshed structure has the minimum size of 0.0307 mm and maximum size of 3.07 mm, and meshing statistics along with a 34 and 35 below. Only difference between the two tensile and flexural structures are the layering stack orientation, and a slight difference if 1 mm in thickness owning to the tensile model having fewer number of layers. As a result of that, the type of element for meshing the both structures are identical. The meshing statistics and plot on the tensile structure is depicted in Figure 3.7 and Figure 3.8 illustrates the meshing plot of the flexural model, followed by the meshing statistics shown in Figure 3.9.

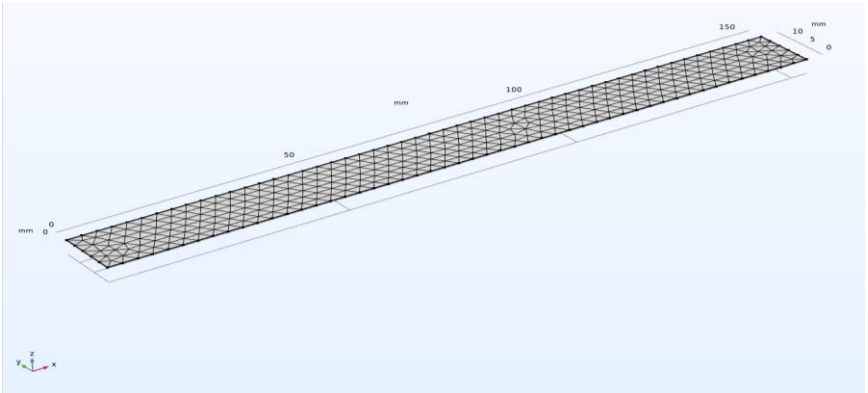

Complete mesh

Mesh vertices:	360
Element type:	All elements
Triangles:	608
Edge elements:	110
Vertex elements:	6

Face element statistics

Number of elements:	608
Minimum element quality:	0.6673
Average element quality:	0.9175
Element area ratio:	0.544
Mesh face area:	2150 mm²

Figure 3.8: Meshing plot and statistics of the tensile specimen. The dimension of the smallest and biggest mesh is the same as the flexural model

Figure 3.9: Mesh statistics for flexural element

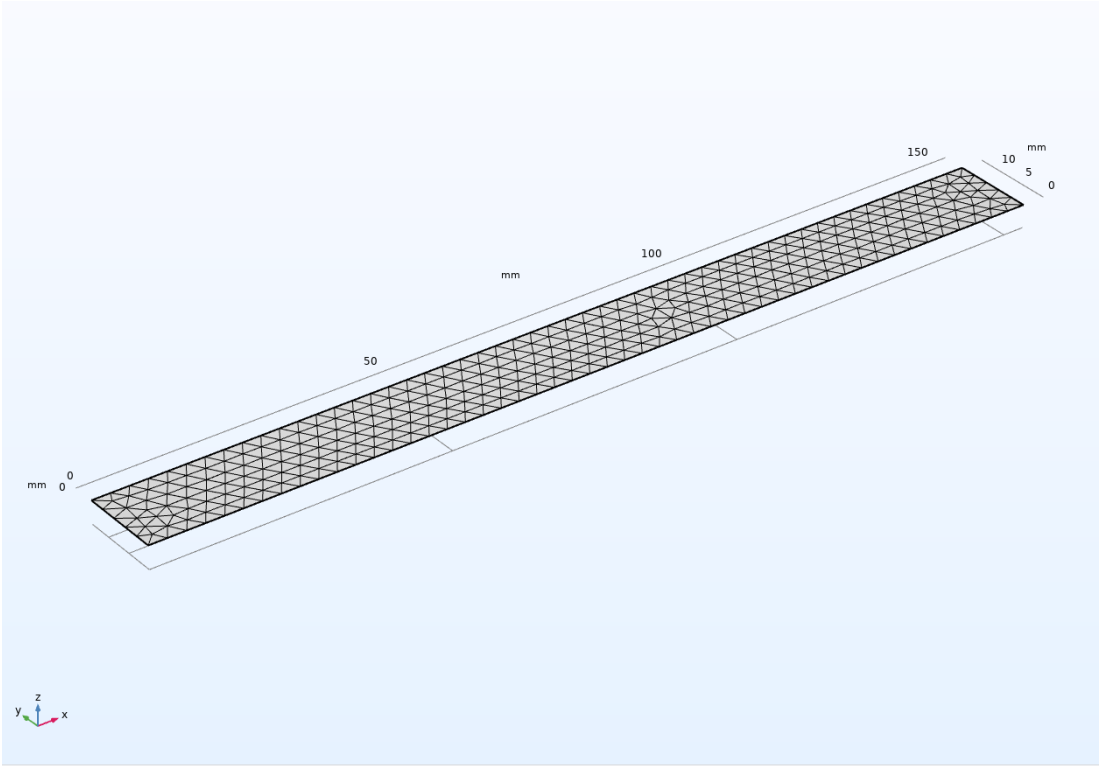

Figure 3.10: Meshing sequence implemented on the structure

3.6 Chapter Review

In the chapter 3 of the thesis, the means of making the FEM simulation is presented which is within the COMSOL multi-physics environment. The mathematical theory in which the modelling is structured is explained with the mathematical operation and equations which govern the modelling of composite materials in COMSOL multi-

physics. Furthermore, the modelling assumptions in which modelling was undertaken is stated and ultimately, the meshing type and statistics are shown.

Chapter 4

RESULTS

4.1 Finite Element Modelling on COMSOL Multiphysics

The results from the FEA were extracted from COMSOL Multiphysics software and both flexural and tensile simulated structures underwent a uniformed total force as a boundary load and a simulated two-point flexural test at two key point in the mid span of the both sides of the flexural test were enforced, respectively (Figure 4.1 and 4.2). Furthermore, even though in real life applications of a tensile test, mostly the specimen has dog bone shape geometry. However, in this simulation, the uniformly shaped rectangular portion of the typical dog bone specimen were considered. Correspondingly, in the flexural test, the rectangular length between the 3-point flexural (bending) test was measured for the FEM analysis of the flexural test. Each specimen was simulated under the assumption of zero degree of freedom within the fixed point. Owning to the fact that the tensile specimen has a fewer number of layers compared to flexural model each model has a different number of applied mesh for FEM calculation to be executed. In COMSOL Multiphysics, there are two general methods of meshing, either physics based or user-controlled method. For both structures, for the sake of better convergence and optimality in processing the results, triangular user defined meshing was considered. Furthermore, the dimensions of each mesh was set to be as miniature as possible to be able to bear more accurate and precise results. Thereafter, results of displacement of structure, von mises stresses,

displacement and strain of structure, along with first principal stresses are depicted. And an evaluation with previous works will be included.

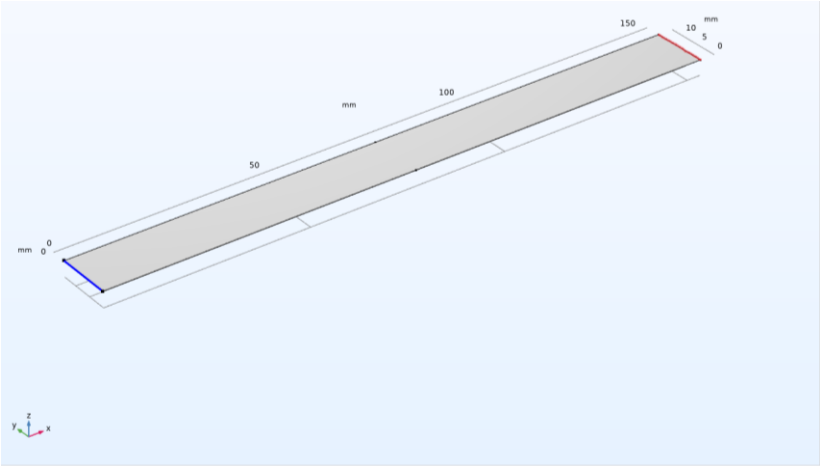

Figure 4.1: Tensile specimen boundary setting, where the blue line is the fixed end and the red line indicates the boundary where the total force of 559.9 MPa which was applied

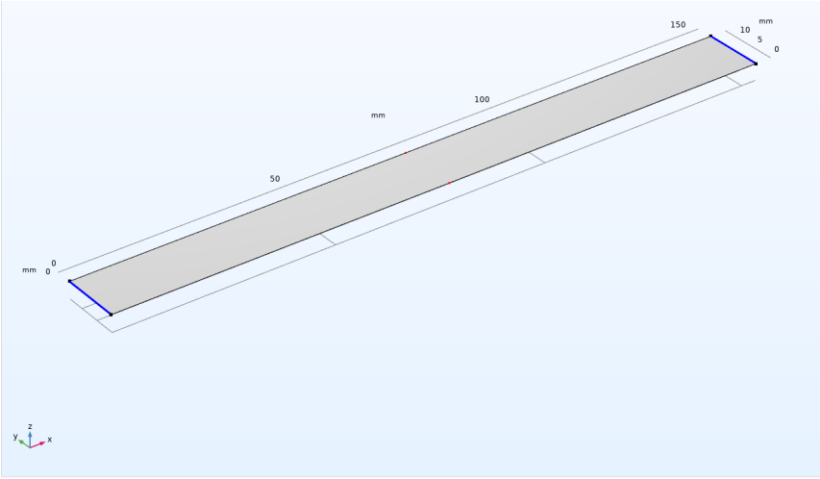

Figure 4.2: Boundary setting of the structure with red dots in the mid-point of the structure indicating the two spots where flexural loads were applied and blue lines as constraints

4.2 Flexural Model Two Point Simulation Result

The flexural model that was assembled as a 32-layer structure consistent of commercial materials known as ONYX material defined as the matrix phase and transverse carbon fiber epoxy (AS4 carbon fiber yarns) as the reinforming phase.

There exists 4 layers of ONYX materials on top of the structure and 4 layers of ONYX at the bottom, which accounts to overall 8 layers of ONYX material and 24 layers of carbon fiber epoxy in between. The dimensions of the structure are 153.6 millimeters of length, 14 mm of width and 4 mm of height under two-point loads of 302.70 MPa load on each point. The model has a 100% infill density and a solid infill pattern. three-dimensional view of the layered structure is further depicted in the Figure 4.3.

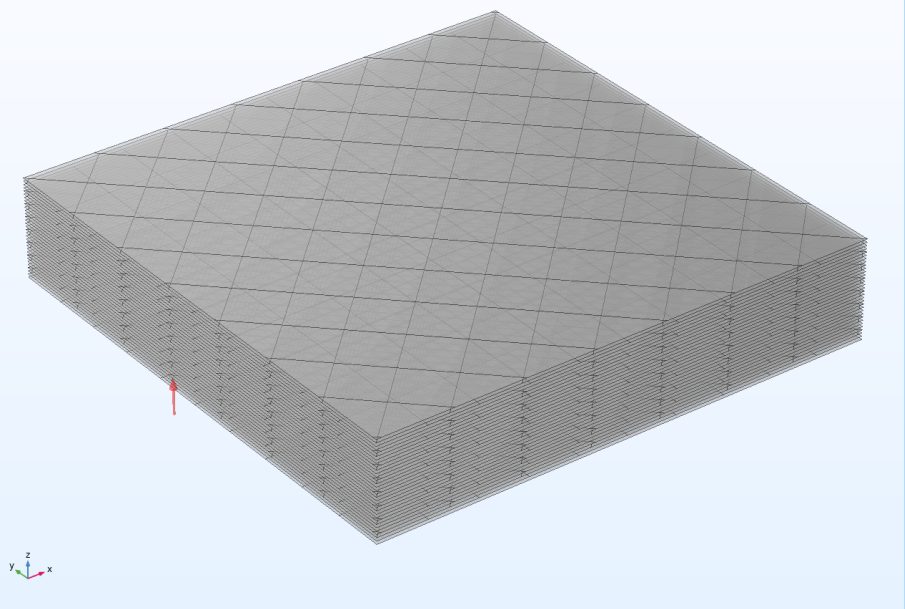

Figure 4.3: 3-dimensional view of the layered flexural structure

After the simulation was executed, it was evaluated that the flexural model had total strain energy is 1.6406 joules and total reaction force of x= 7.5982E-9, y= 3.4136E-9, z= -605.40. Depending on the displacement and the curvature spotted within the structure, it was noted that the four ONYX layers placed on the top and the bottom were the most resilient compared to carbon fiber layers owning to their superior mechanical properties. However, depending on the orientation sequence in which layers were stacked upon each other, it is bordered that the layer number five, which is the first carbon fiber layer is the layer which underwent the most stresses and

deflection. Layer number five is oriented at a 0 degree with respect to the reference coordinate system and is the boundary layer between ONYX material and the reinforcement phase. However, same occurrence did not happen to the last reinforcing layer (layer 28) as it did not bear the same amount of stress within the body of the layered material. Needless to say, that layer 28 is oriented at 45 degrees with respect to the reference axis. Furthermore, the amount of displacement and through the thickness, first principal stresses and also and evaluation of von mises stresses on 6 key points within the structure. The defining points on the coordinate of $[x = 0, y = 0]$ for point one, $[x = 0, y = 14]$ for point 2, $[x = 76.8, y = 0]$ for point, [x=76.8, y= 14] for point 4, $[x = 153.6, y = 0]$ for point 5 and [x=153.6, y= 14] for point 6. Needless to say, since the coordinate is through the thickness, all the layers underneath the defined point are considered (Figure 4.4 to Figure 4.10).

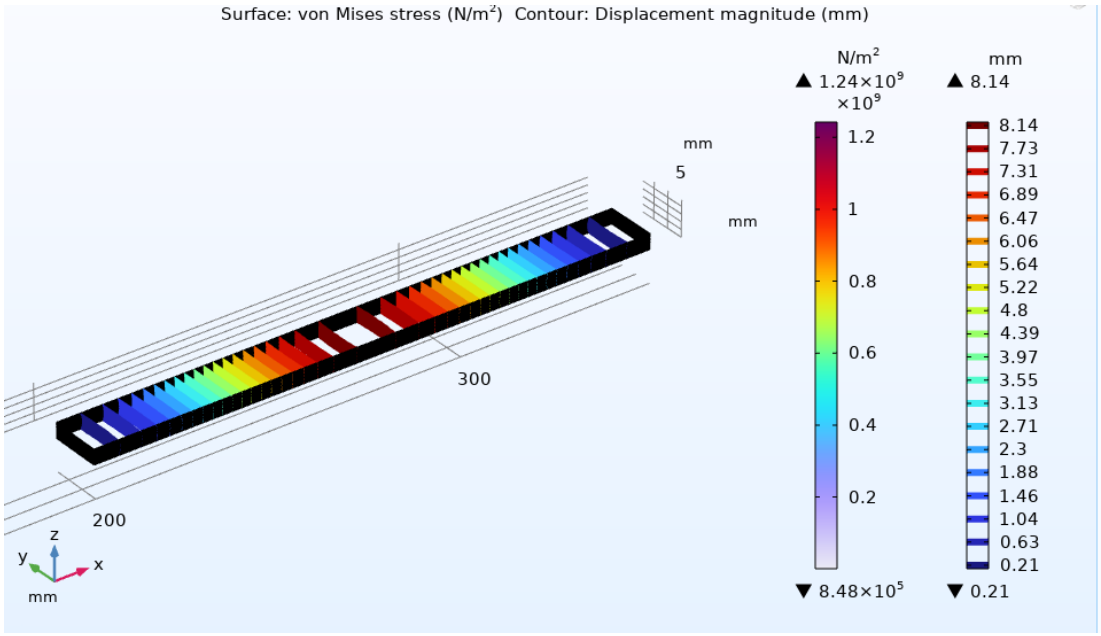

Figure 4.4: View of flexed structure from above

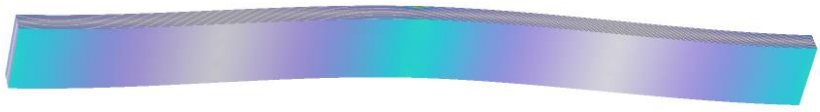

Figure 4.5: View of the curved flexural structure from the bottom

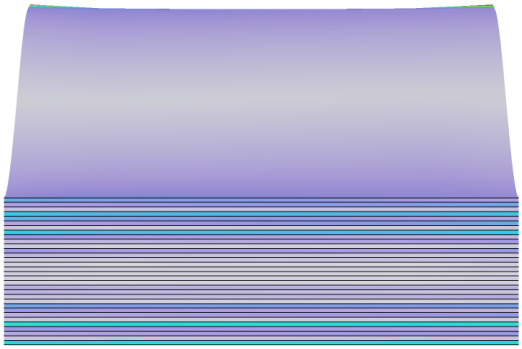

Figure 4.6: Widthwise view of the layered structure

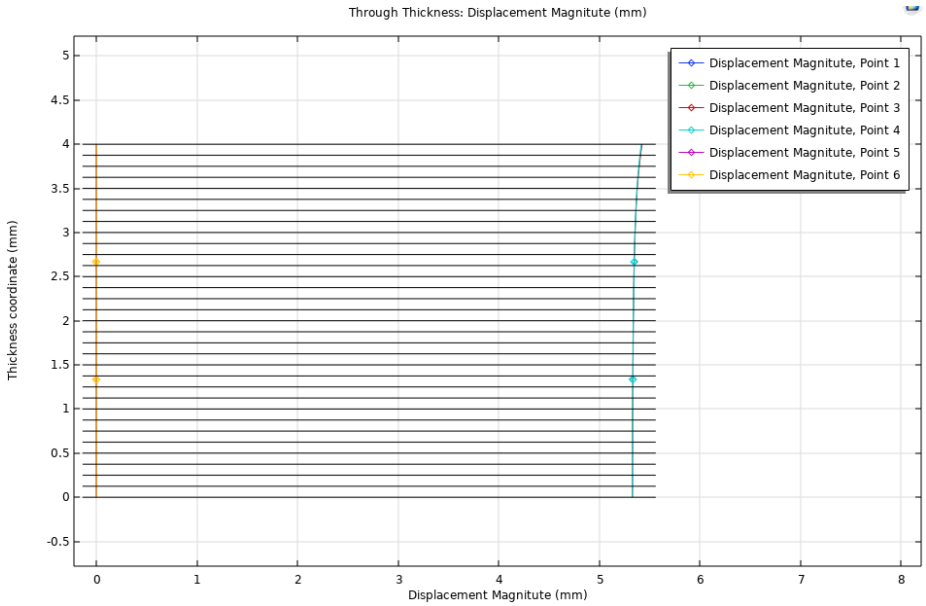

Figure 4.7: Displacement curve of the structure in millimeters6 key points the defining points on the coordinate of $[x = 0, y = 0]$ for point one, $[x = 0, y = 16]$ for point 2, $[x = 76.8, y = 0]$ for point, [x=76.8, y= 14] for point 4, $[x = 157.6, y = 0]$ for point 5 and [x=157.6, y= 14] for point 6. Each black solid line indicates a layer

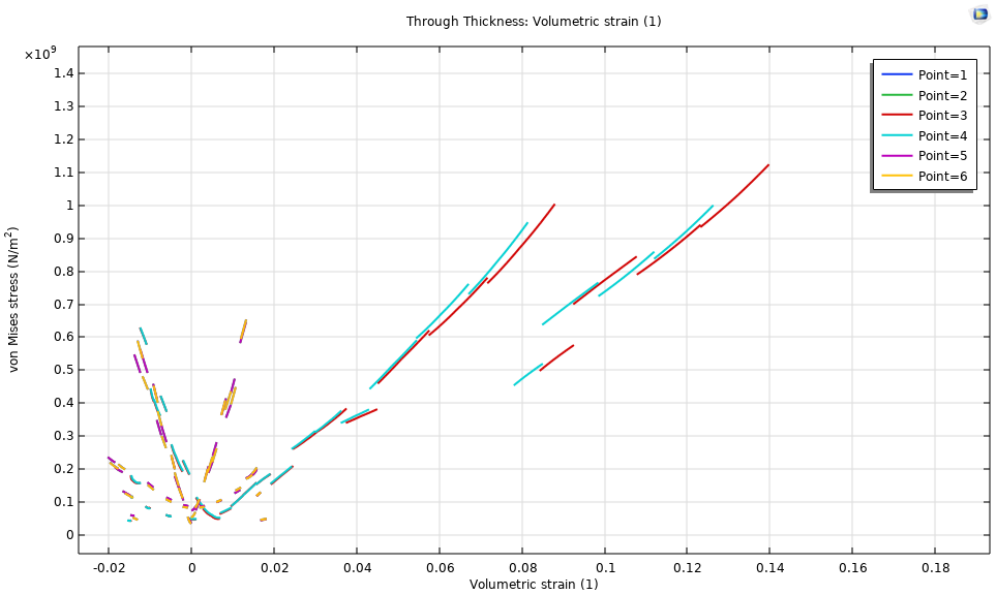

Figure 4.8: Volumetric strain to von mises stress 6 key points the defining points on the coordinate of $[x = 0, y = 0]$ for point one, $[x = 0, y = 16]$ for point 2, $[x = 76.8, y = 0]$ for point, [x=76.8, y= 14] for point 4, $[x = 157.6, y = 0]$ for point 5 and [x=157.6, y= 14] for point 6

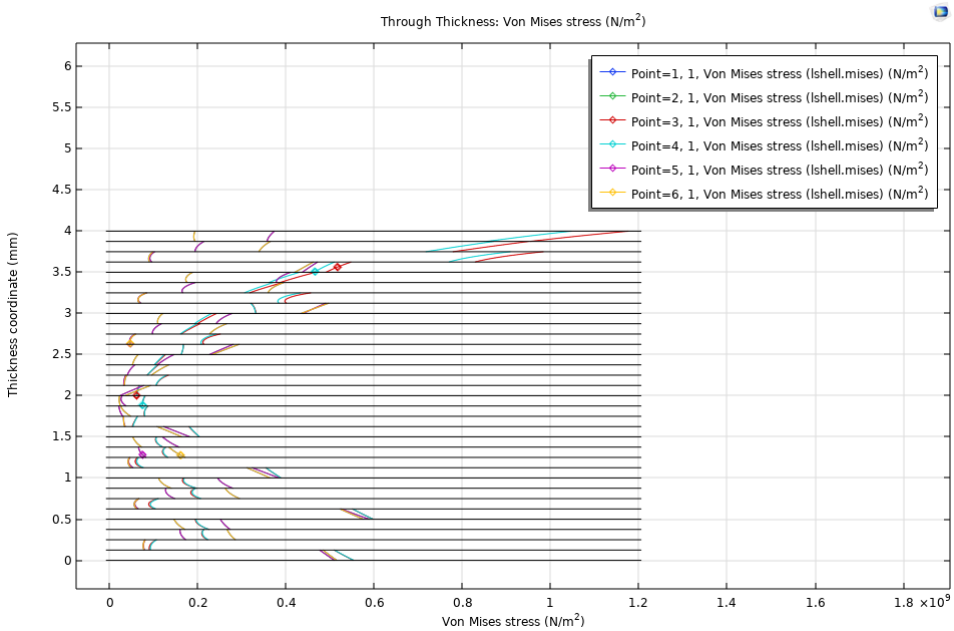

Figure 4.9**:** von mises stresses of 6 key points the defining points on the coordinate of $[x = 0, y = 0]$ for point one, $[x = 0, y = 16]$ for point 2, $[x = 76.8, y = 0]$ for point, [x=76.8, y= 14] for point 4, $[x = 157.6, y = 0]$ for point 5 and [x=157.6, y= 14] for point 6. Needless to say, since the coordinate is through the thickness, all the layers underneath the defined point are considered

As it is shown on the Figure 26, there are two main pressure point that the flexural loads were applied. One at the location of (x=76.8 and y= 0) and (x=76.8 and y=14).

In the first mentioned point, the maximum von mises recorded stress was 1.1968E9 newton per square meter, however, the amount of maximum stress recorded on the second point was recorded to be 1.1222E9 newton per square meter, moreover, as it is depicted, compared to other layers, layer number 4 sustained more stress which was recorded to be 5.0299E8 newton per square meter.

4.3 Tensile Model Simulation Results

The prepared tensile model was set to have dimensions of 157 millimeters in length, 16 millimeters in width and 3 millimeters in Hight. Differences in the width of the specimen is due to the fact that each layer of specimen are set to be 0.125 millimeters and the tensile models has 24 layers. The model has an infill ratio of 100 percent and solid infill pattern. Moreover, the model had the overall elastic strain of 29.41589 joules and the global reaction forces were evaluated as x= -23515.80, y = -4.2122E-9 z= 7.5562E-6. The tensile model has a fixed constraint with zero degrees of freedom and a uniformly spread boundary load enforced on the opposite side of the structure with the magnitude total force of 599.9 MPa (Figure 21). The amount of global reaction forces in the constraint boundary, the middle and the load enforced boundary are depicted in a 6-point plot of von mises stresses with, The defining points on the coordinate of $[x = 0, y = 0]$ for point one, $[x = 0, y = 16]$ for point 2, $[x = 78.5, y = 0]$ for point, [x=78.5, y= 16] for point 4, $[x = 157, y = 0]$ for point 5 and [x=157, y= 14] for point 6. Needless to say, since the coordinate is through the thickness, all the layers underneath the defined point are considered.

After the aforementioned uniformed boundary load was applied on the tensile structure, as expected, the ONYX material shown better resilience towards the stress and remained relatively intact. However, the mechanical behavior of the reenforcing

phase did not play out in the same manner as the ONYX phase. Amongst the carbon fiber layers, most critically behaved layers were layers with a 90-degree orientation with respect to the reference orientation. Which were layers numbers 5,9,13,17. However, even between the aforementioned four layers, layer 13 and 17 on the side constraint boundary, bore more stress in general (1.6521E9 and 1.4978E9 $\frac{N^2}{M}$ respectively). The other group of reinforcing layers which underwent more stress, where layers oriented at 0 degree with respect to the reference coordinate system. Although the 0-degree layers did not experience the same amount of stress as the -90-layer group. In the following, a view of the deflected structure, from the side, and another image from the constrained face of the structure is depicted for proper inspection of the structure from the most important angles. Thereafter, through the thickness displacement, von mises stresses and overall volumetric strain are shown in Figures 4.11, 4.12 and 4.13 and 4.14 respectively.

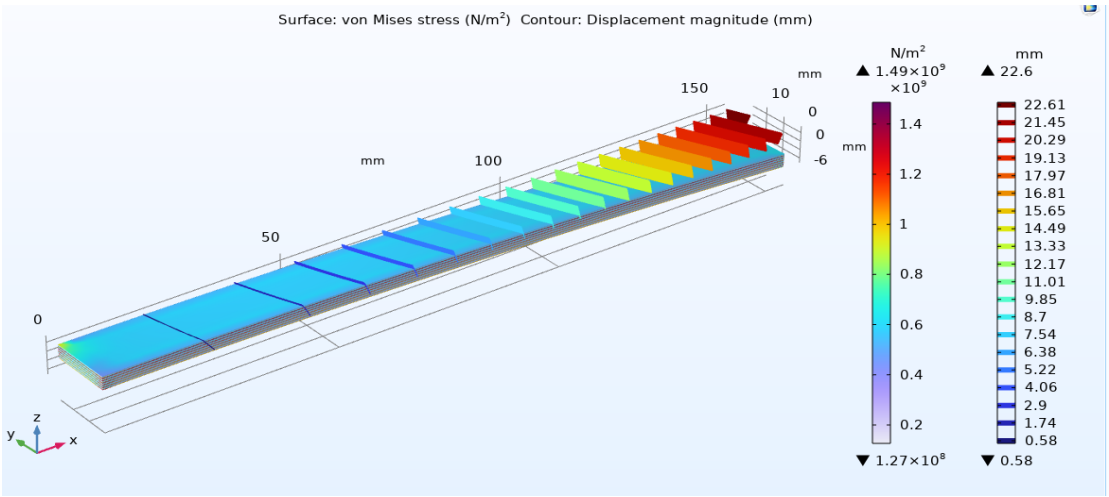

Figure 4.10: Tensile stress and displacement values

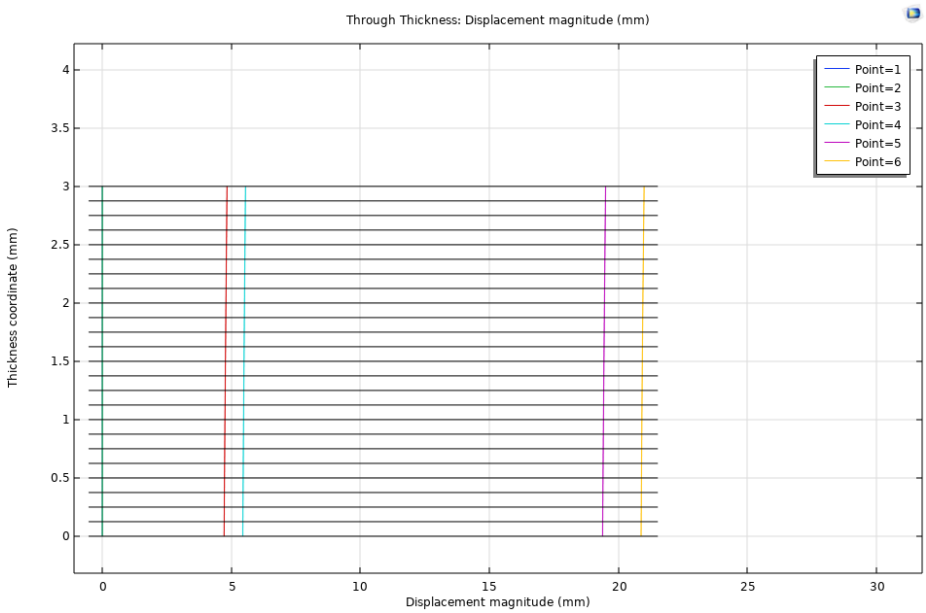

Figure 4.11: Through the thickness displacement

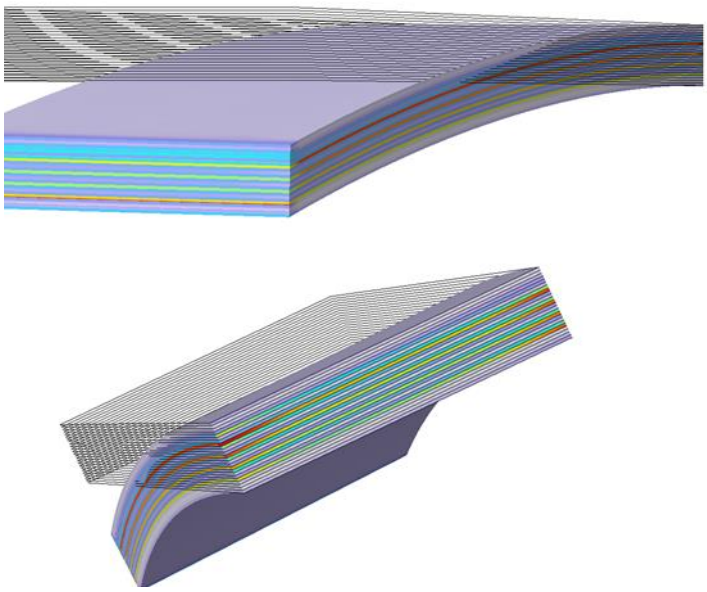

Figure 4.12: Von mises stresses and different orientation views of the structure

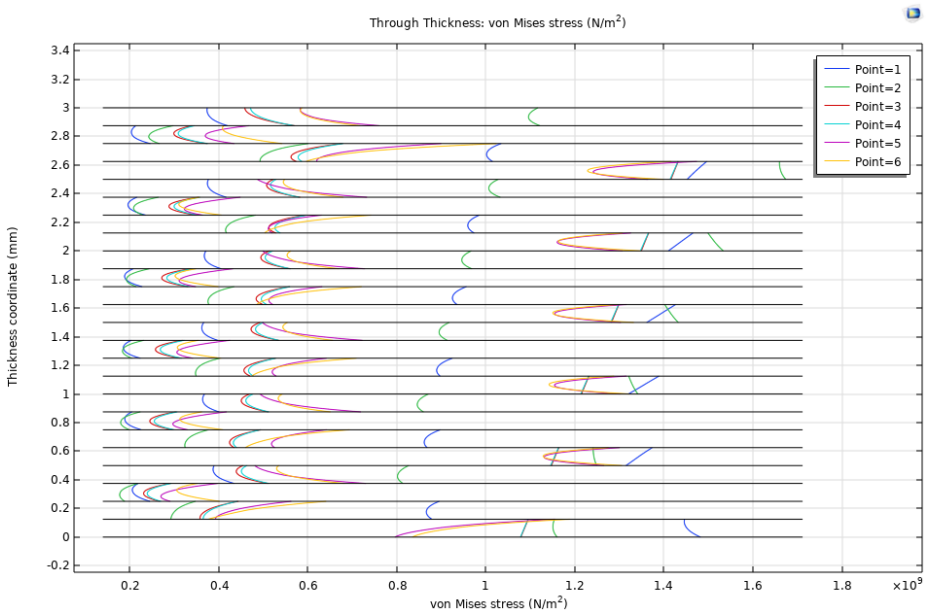

Figure 4.13: Von mises stresses, The defining points on the coordinate of $[x = 0, y = 0]$ for point one, $[x = 0, y = 16]$ for point 2, $[x = 78.5, y = 0]$ for point, [x=78.5, y= 16] for point 4, $[x = 157, y = 0]$ for point 5 and [x=157, y= 14] for point 6. Needless to say, since the coordinate is through the thickness, all the layers underneath the defined point are considered

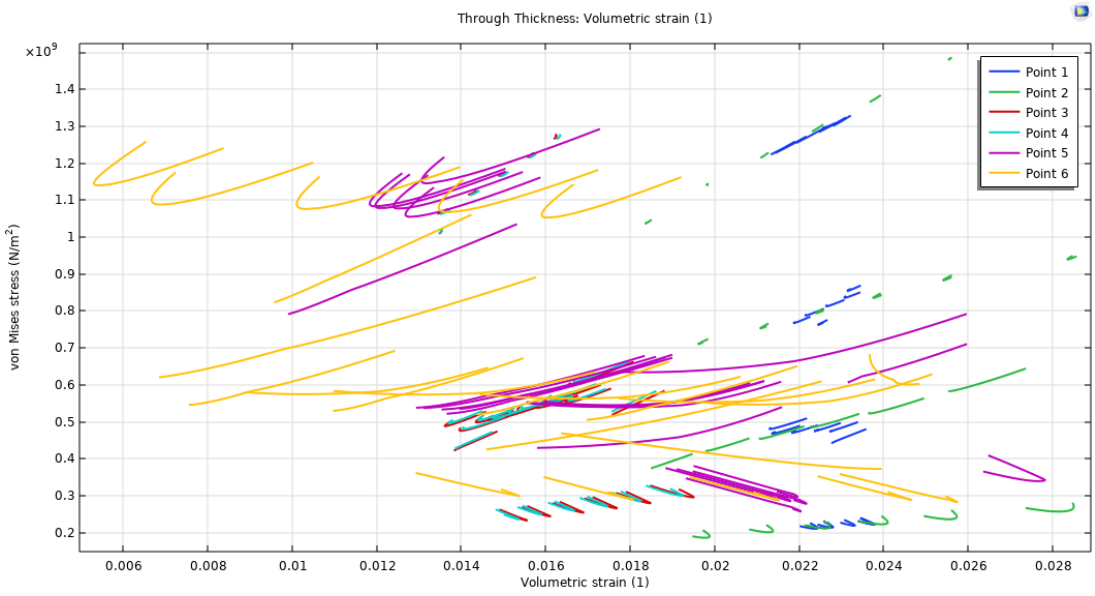

Figure 4.14: Volumetric strain to von mises within the 6-key points

4.5 Validation and Comparison

In the process of implementing the flexural and tensile stress generated within the separate structures, the mechanical properties of both type of structures are recorded

and, in this section, they are compared to the most similar previous research undertaken before. In a research done by Ghebretinsae et al [60], samples with the same defined material were generated, using ONYX material and AS4 carbon fiber as reinforming phase of the structure. The mechanical properties imported form their FEA modelling is depicted in Table 4.1.

Based on the suggestion made by the investigation carried out by Parmiggiani et al [61], the fiber orientation, fiber stacking sequence and the number of layers from is adopted from Parmiggiani's work, while still using the same defined material ,infill pattern and ratio and same point load and boundary load for flexural and tensile model respectively. As the results of the simulation shown, the maximum stress for the newly structured models is recorded to be 1.490E9 $\frac{N^2}{M}$ for the flexural model and 1.240E9 $\frac{N^2}{M}$ for the tensile model respectively, which is an improvement compared to the previous results. Furthermore, the amount of displacement in the tensile specimen was recorded to be 0.3 mm and 4 mm for the flexural structure which is significantly better and is compared in the Table 4.2 below.

Table 4.1: Results from the simulation done by Ghebretinsae et al. [60]

Type of test	Load applied	Results of FEM displacement [mm]	Max stress [MPa]
Tensile test	559.9 MPa (as a total boundary load)	1.13	470.5
Flexural test	302.70 N (at two points)	9.14	254.1

Table 4.2: Results from the simulation done via COMSOL Multiphysics

Type of test	Load applied	Results of FEM displacement[mm]	Max stress [MPa]
Tensile test	559.9 MPa (as a total boundary load)	22.6	1490
Flexural test	302.70 N (at two points)	8.14	1240

4.6 Discussion

A finite element Modeling process was undertaken on two separate simulated structures. the structures have A4S carbon fiber as reinforcement agent and commercial material known as ONYX material in the form of the matrix phase of the both tensile and flexural structures. the models were generated within the COMSOL multi- physics. the materials were assumed under the circumstances of perfect binding and no delamination. furthermore, the simulated material is free of any void and entrapped air and the condition of perfect bonding stands. as a result, in the COMSOL multi-physics, the layer shelled interface was chosen to simulate the layered nature of the 3D printed structure and the mechanical properties of the carbon fiber reinforcement and the matrix material was defined based on the values and assumptions in the research done by Ghebretinsae et al as was pointed out that the composites material manufactured with Novel 3D printing possess unprecedented mechanical properties. Furthermore, owning to the change in layer orientation and sequencing the novel simulated material shown improved mechanical properties. Based upon the results extracted from the work done by Bárnik et al [73], It's best to stack the layers at even numbers as odd numbers lead to structures failing more often

and it is recommended to use even numbered layers for 3D printing applications. furthermore, it was determined that samples with higher infill density yielded better tensile properties. Moreover, as was mentioned in the previous section related to the results from tensile and flexural, ONYX layered phases depicted superior mechanical properties compared to carbon fiber phase and depending on the layer orientation and the orientation of the layers above and below somewhat plays a role in the state of stress within the structures as is shown in the figures in the aforementioned sections and the point evaluation done on the bending point in the flexural structure where the quantity of maximum von mises slightly varied on each bending point.

4.7 Chapter Review

In this final chapter, the process of simulation under the aforementioned conditions was undertaken and the results of displacements, stress and strains within the structures underwent tensile and two point flexural (bending) are evaluated. Furthermore, the aftermath of the simulation is compared to previous work of similar background and aside from stacking orientation and sequence, all the parameters are held in identical circumstances. However, the aforesaid changes resulted in improved tensile and flexural resistance of the structures.

Chapter 5

CONCLUSION

In essence, this thesis was an investigation in improving the flexural and tensile capabilities of FFF parts which is a technique in AM. They are one of the most important factors in having capable and reliable parts in practical applications. There are many aspects in which composite manufacturing via AM techniques could be modified, namely the bonding quality between layers, raster angle and orientation, compensating with offset parts and etc. However, non-manufacturing related parameters such as the layer stacking orientation and orientation can be very impactful and they were investigated in this thesis via a FEM simulation adopted by previous existing results. Owning to the precise control in AM and little to no constraint in term of design geometry and topology, structures could have certain infill density and pattern best suited to the direction of specific stresses applied to them and this leads to less material usage and time and resource saving. However, in applications where there could be random and stochastic stresses, the option of having less density becomes a liability in terms of dealing with the aforesaid random forces, even though that takes more time and material to fabricate the material. As a result of that, in this thesis, for the sake of versatility of usage of the proposed material, a solid infill pattern and 100% infill ratio was chosen. Moreover, as stacking sequence and layer orientation is very important in fiber reinforced structural materials, an attempt to change the orientation and stacking order was made. Two types of materials were simulated, ONYX material which are chopped CF materials, served as the matrix phase for both tensile and

flexural simulated specimen and AS4 carbon yarns with 34.5% of their mechanical properties as reinforcing fiber. The change in the aforesaid parameters resulted in improved maximum stress compared to previous similar work. Referring to tables 4 and 5, in the previous work, the tensile test Max stress was 470.5 [MPa], and flexural test Max stress of 254.1 [MPa]. Overall, following conclusions are made;

- ONYX layered phases depicted superior mechanical properties compared to carbon fiber phase in flexural model
- ONYX layered phases were more vulnerable in tensile simulation.
- Carbon fiber reinforcements underwent more stress in upper layers in the tensile simulation.
- Depending on the layer orientation and the orientation of the layers above and below of each laminate, the state of stress within the aforementioned sections varied.
- Changes made in stacking orientation and stacking sequence, resulted in improved tensile and flexural resistance of the structures.
- Some layers endured significantly more stress while some layers remained relatively dormant.

In the future works, possibilities to fabricate composite materials where all layers used within the layered structure could play a more load bearing part even though having a multi orientated layer structure is a subject where more investigations should be made. under the new circumstances, the maximum stress for tensile test was recorded to be 1490 [MPa] and flexural to be 1240 [MPa] showing significant improvement given the assumptions made to undertake the simulation.

REFERENCES

[1] Dixit US, Hazarika M, Davim JP. Manufacturing through ages 2017:99–125. https://doi.org/10.1007/978-3-319-42916-8_5.

[2] Choudhari CJ, Thakare PS, Sahu SK. 3D printing of composite sandwich structures for aerospace applications 2022:45–73. https://doi.org/10.1007/978-981-16-7377-1_3.

[3] Whenish R, Velu R, Anand Kumar S, Ramprasath LS. Additive manufacturing technologies for biomedical implants using functional biocomposites 2022:25–44. https://doi.org/10.1007/978-981-16-7377-1_2.

[4] Jandyal A, Chaturvedi I, Wazir I, Raina A, Ul Haq MI. 3D printing – A review of processes, materials and applications in industry 4.0. Sustain Oper Comput 2022;3:33–42. https://doi.org/10.1016/J.SUSOC.2021.09.004.

[5] Sandström CG. The non-disruptive emergence of an ecosystem for 3D Printing - Insights from the hearing aid industry's transition 1989-2008. Technol Forecast Soc Change 2016;102:160–8. https://doi.org/10.1016/j.techfore.2015.09.006.

[6] Jain PK, Jain PK. Use of 3D printing for home applications: A new generation concept. Mater Today Proc 2021. https://doi.org/10.1016/j.matpr.2020.12.145.

[7] Bi K, Lin D, Liao Y, Wu C-H, Parandoush P. Additive manufacturing embraces big data. Prog Addit Manuf 2021. https://doi.org/10.1007/s40964-021-00172-

8.

[8] Mahamood RM, Akinlabi ET. Laser additive manufacturing. 3D Print. Break. Res. Pract., IGI Global; 2016, p. 154–71. https://doi.org/10.4018/978-1-5225-1677-4.ch008.

[9] Leary M. Design for additive manufacturing. Elsevier; 2019. https://doi.org/10.1016/C2017-0-04238-6.

[10] Ali SF, Malik FM, Kececi EF, Bal B. Optimization of additive manufacturing for layer sticking and dimensional accuracy, 2019, p. 185–98. https://doi.org/10.4018/978-1-5225-9167-2.ch009.

[11] Rias AL, Bouchard C, Segonds F, Vayre B, Abed S. Design for additive manufacturing: Supporting intrinsic-motivated creativity. Emot. Eng. Vol.5, Springer International Publishing; 2017, p. 99–115. https://doi.org/10.1007/978-3-319-53195-3_8.

[12] Provaggi E, Kalaskar DM. 3D printing families: Laser, powder, nozzle based techniques. 3D Print. Med., Elsevier Inc.; 2017, p. 21–42. https://doi.org/10.1016/B978-0-08-100717-4.00003-X.

[13] Gaisford S. 3D printed pharmaceutical products. 3D Print. Med., Elsevier Inc.; 2017, p. 155–66. https://doi.org/10.1016/B978-0-08-100717-4.00007-7.

[14] Capelli C, Schievano S. Computational analyses and 3D printed models: A

combined approach for patient-specific studies. 3D Print. Med., Elsevier Inc.; 2017, p. 73–90. https://doi.org/10.1016/B978-0-08-100717-4.00005-3.

[15] Roopavath UK, Kalaskar DM. Introduction to 3D printing in medicine. 3D Print. Med., Elsevier Inc.; 2017, p. 1–20. https://doi.org/10.1016/B978-0-08-100717-4.00001-6.

[16] Sima F, Sugioka K, Vázquez RM, Osellame R, Kelemen L, Ormos P. Three-dimensional femtosecond laser processing for lab-on-a-chip applications. Nanophotonics 2018;7:613–34. https://doi.org/10.1515/nanoph-2017-0097.

[17] Mishra PK, Senthil P, Adarsh S, Anoop MS. An investigation to study the combined effect of different infill pattern and infill density on the impact strength of 3D printed polylactic acid parts. Compos Commun 2021;24:100605. https://doi.org/10.1016/j.coco.2020.100605.

[18] Agrawaal H, Thompson JE. Additive manufacturing (3D Printing) for analytical chemistry. Talanta Open 2021:100036. https://doi.org/10.1016/j.talo.2021.100036.

[19] Parmar H, Khan T, Tucci F, Umer R, Carlone P. Advanced robotics and additive manufacturing of composites: towards a new era in Industry 4.0. Https://DoiOrg/101080/1042691420201866195 2021;37:483–517. https://doi.org/10.1080/10426914.2020.1866195.

[20] Venugopal V, McConaha M, Anand S. Integration of design for additive

manufacturing constraints with multimaterial topology optimization of lattice structures for optimized thermal and mechanical properties. J Manuf Sci Eng Trans ASME 2022;144. https://doi.org/10.1115/1.4052193/1115886.

[21] Ngo TD, Kashani A, Imbalzano G, Nguyen KTQ, Hui D. Additive manufacturing (3D printing): A review of materials, methods, applications and challenges. Compos Part B Eng 2018;143:172–96. https://doi.org/10.1016/j.compositesb.2018.02.012.

[22] Pazhamannil RV, Govindan P. Current state and future scope of additive manufacturing technologies via vat photopolymerization. Mater Today Proc 2021. https://doi.org/10.1016/j.matpr.2020.11.225.

[23] Richter S, Wischmann Iit-Berlin S. Additive manufacturing methods-state of development, market prospects for industrial use and ICT-specific challenges in research and development A study within the scope of scientific assistance for the AUTONOMICS for Industry 4.0 technology programme of the Federal Ministry for Economic Affairs and Energy 2. n.d.

[24] Chen C, Wang X, Wang Y, Yang D, Yao F, Zhang W, et al. Additive manufacturing of piezoelectric materials. Adv Funct Mater 2020;30:1–29. https://doi.org/10.1002/adfm.202005141.

[25] Der Klift F Van, Koga Y, Todoroki A, Ueda M, Hirano Y, Matsuzaki R. 3D Printing of continuous carbon fibre reinforced thermo-plastic (CFRTP) tensile test specimens. Open J Compos Mater 2016;06:18–27.

https://doi.org/10.4236/ojcm.2016.61003.

[26] Gebisa AW, Lemu HG. Materials investigating effects of fused-deposition modeling (FDM) processing parameters on flexural properties of ULTEM 9085 using designed experiment n.d. https://doi.org/10.3390/ma11040500.

[27] Kumar R, Singh R, Ahuja IS. Joining of 3D printed dissimilar thermoplastics with consumable tool through friction stir spot welding: a case study. encycl renew sustain mater 2020:91–6. https://doi.org/10.1016/b978-0-12-803581-8.11529-2.

[28] Sai T, Vimal ·, Pathak K, Srivastava AK. Modeling and optimization of fused deposition modeling (FDM) process through printing PLA implants using adaptive neuro-fuzzy inference system (ANFIS) model and whale optimization algorithm. J Brazilian Soc Mech Sci Eng 2020;42:617. https://doi.org/10.1007/s40430-020-02699-3.

[29] Gao X, Yu N, Li J. Influence of printing parameters and filament quality on structure and properties of polymer composite components used in the fields of automotive. Struct Prop Addit Manuf Polym Components 2020:303–30. https://doi.org/10.1016/B978-0-12-819535-2.00010-7.

[30] Levy GN, Schindel R, Kruth JP. Rapid manufacturing and rapid tooling with layer manufacturing (LM) technologies, state of the art and future perspectives. CIRP Ann - Manuf Technol 2003;52:589–609. https://doi.org/10.1016/S0007-8506(07)60206-6.

[31] Pilipović A, Raos P, Šercer M. Experimental analysis of properties of materials for rapid prototyping. Int J Adv Manuf Technol 2009;40:105–15. https://doi.org/10.1007/s00170-007-1310-7.

[32] Estermann LWS-J. 2018_Mechanical-properties-of-fused-deposition-modeling-fdm-3d-printing-materials.pdf. RTejournal - Forum FurRapid technologie; n.d. https://doi.org/0009-2-47812.

[33] Kajimoto J, Koyanagi J, Maruyama Y, Kajita H, Matsuzaki R. Automated interlaminar reinforcement with thickness directional fiber arrangement for 3D printing. Compos Struct 2022;286:115321. https://doi.org/10.1016/j.compstruct.2022.115321.

[34] Sandhu GS, Boparai KS, Sandhu KS. Influence of slicing parameters on selected mechanical properties of fused deposition modeling prints. Mater Today Proc 2021;48:1378–82. https://doi.org/10.1016/j.matpr.2021.09.118.

[35] Gavali VC, Kubade PR, Kulkarni HB. Mechanical and thermo-mechanical properties of carbon fiber reinforced thermoplastic composite fabricated using fused deposition modeling method. Mater Today Proc 2019;22:1786–95. https://doi.org/10.1016/j.matpr.2020.03.012.

[36] Ichihara N, Ueda M, Urushiyama Y, Todoroki A, Matsuzaki R, Hirano H. Progressive damage simulation for a 3D-printed curvilinear continuous carbon fiber-reinforced thermoplastic based on continuum damage mechanics. Adv Compos Mater 2020;29:459–74.

https://doi.org/10.1080/09243046.2020.1724430.

[37] Shiratori H, Todoroki A, Ueda M, Matsuzaki R, Hirano Y. Mechanism of folding a fiber bundle in the curved section of 3D printed carbon fiber reinforced plastics. Adv Compos Mater 2020;29:247–57. https://doi.org/10.1080/09243046.2019.1682794.

[38] Khan I, Kumar N. Fused deposition modelling process parameters influence on the mechanical properties of ABS: A review. Mater Today Proc 2020;44:4004–8. https://doi.org/10.1016/j.matpr.2020.10.202.

[39] Shaffer GD. An archaeomagnetic study of a wattle and daub building collapse. Http://DxDoiOrg/101179/009346993791974334 2013;20:59–75. https://doi.org/10.1179/009346993791974334.

[40] Creep and shrinkage prediction model for analysis and design of concrete structures - model B3 — Northwestern Scholars n.d. https://www.scholars.northwestern.edu/en/publications/creep-and-shrinkage-prediction-model-for-analysis-and-design-of-c-2 (accessed February 23, 2022).

[41] John Wiley & Sons. Reinforced Concrete Structures - Robert Park, Thomas Paulay - Google Books. A wiley-interscience Publ 1975. https://books.google.com.cy/books?hl=en&lr=&id=QPDvchXv5zUC&oi=fnd&pg=PA1&ots=_0MU9huXmw&sig=85MgsQrjkl-6PMGJmUt9CHKtN1A&redir_esc=y#v=onepage&q&f=false (accessed February 23, 2022).

[42] Krishan K. Chawla. Composite Materials: Science and Engineering - Krishan K. Chawla - Google Books. Springer new york heidelb london 2012. https://books.google.com.cy/books?hl=en&lr=&id=rbuNxwzM27cC&oi=fnd&pg=PR7&ots=UpgPusNgi4&sig=soJFrMs_alKj3NjT8OeG_glUwvk&redir_esc=y#v=onepage&q&f=false (accessed February 24, 2022).

[43] Egbo MK. A fundamental review on composite materials and some of their applications in biomedical engineering. J King Saud Univ - Eng Sci 2021;33:557–68. https://doi.org/10.1016/J.JKSUES.2020.07.007.

[44] Jayan JS, Appukuttan S, Wilson R, Joseph K, George G, Oksman K. An introduction to fiber reinforced composite materials. Fiber Reinf Compos 2021:1–24. https://doi.org/10.1016/B978-0-12-821090-1.00025-9.

[45] Pegoretti A. Towards sustainable structural composites: A review on the recycling of continuous-fiber-reinforced thermoplastics. Adv Ind Eng Polym Res 2021;4:105–15. https://doi.org/10.1016/J.AIEPR.2021.03.001.

[46] An Introduction to Materials Engineering and Science for Chemical and ... - Brian S. Mitchell - Google Books n.d. https://books.google.com.cy/books?hl=en&lr=&id=iQQcERxsNywC&oi=fnd&pg=PR7&ots=GJ5tyXo3C1&sig=0T9X2wZGzn75L1wNhqQHgKvGvrU&redir_esc=y#v=onepage&q&f=false (accessed March 17, 2022).

[47] Ahmed S, Jones FR. A review of particulate reinforcement theories for polymer composites. J Mater Sci 1990 2512 1990;25:4933–42.

https://doi.org/10.1007/BF00580110.

[48] Ishai O, Cohen LJ. Elastic properties of filled and porous epoxy composites. Int J Mech Sci 1967;9:539–46. https://doi.org/10.1016/0020-7403(67)90053-7.

[49] Petersen RC. Discontinuous fiber-reinforced composites above critical length. biomater bioeng rc 2005.

[50] Yamamoto S ichi, Tsutsumi T. The population dynamics of naturally regenerated hinoki seedlings in artificial hinoki stands (III) Dynamics of the seed population on the forest floor. J Japanese For Soc 1984;66:483–90. https://doi.org/10.11519/jjfs1953.66.12_483.

[51] Soutis C. Fibre reinforced composites in aircraft construction. Prog Aerosp Sci 2005;41:143–51. https://doi.org/10.1016/j.paerosci.2005.02.004.

[52] Wang C, Liu G, An Q, Chen M. Occurrence and formation mechanism of surface cavity defects during orthogonal milling of CFRP laminates. Compos Part B Eng 2017;109:10–22. https://doi.org/10.1016/J.COMPOSITESB.2016.10.015.

[53] Che D, Saxena I, Han P, Guo P, Ehmann KF. Machining of carbon fiber reinforced plastics/polymers: A literature review. J Manuf Sci Eng Trans ASME 2014;136. https://doi.org/10.1115/1.4026526/376924.

[54] Altin Karataş M, Gökkaya H. A review on machinability of carbon fiber reinforced polymer (CFRP) and glass fiber reinforced polymer (GFRP)

composite materials. Def Technol 2018;14:318–26. https://doi.org/10.1016/J.DT.2018.02.001.

[55] Bhargava. A. K. Engineering Materials: Polymers, ceramics and composites - A. K. Bhargava - Google Books. PHI Learn Priv Ltd 2012. https://books.google.com.cy/books?hl=en&lr=&id=zbr9vBsbAJYC&oi=fnd&pg=PR1&ots=TKJp7LiLek&sig=zaC6eC_bHk0aseBKzEtoiNOwAGY&redir_esc=y#v=onepage&q&f=false (accessed March 17, 2022).

[56] Liu Y, Zwingmann B, Schlaich M. Carbon fiber reinforced polymer for cable structures—a review. polym 2015, Vol 7, Pages 2078-2099 2015;7:2078–99. https://doi.org/10.3390/POLYM7101501.

[57] Meier U. Carbon Fiber-Reinforced Polymers: Modern materials in bridge engineering. Https://DoiOrg/102749/101686692780617020 2018;2:7–12. https://doi.org/10.2749/101686692780617020.

[58] Bacon Roger. US2957756A - Filamentary graphite and method for producing the same - Google Patents 1960. https://patents.google.com/patent/US2957756A/en (accessed March 17, 2022).

[59] Aleksendrić D, Carlone P. Introduction to composite materials. 2015. https://doi.org/10.1533/9781782421801.1.

[60] Technology E. Faculty of Science and Technology Master ’ s thesis 2019.

[61] Parmiggiani A, Prato M, Pizzorni M. Effect of the fiber orientation on the tensile and flexural behavior of continuous carbon fiber composites made via fused filament fabrication. Int J Adv Manuf Technol 2021;114:2085–101. https://doi.org/10.1007/S00170-021-06997-5/FIGURES/12.

[62] COMSOL Multiphysics® Software - Understanding, Predicting and Optimizing n.d. https://www.comsol.de/comsol-multiphysics (accessed March 4, 2022).

[63]LiveLink™ for MATLAB® 2018. https://doc.comsol.com/5.4/doc/com.comsol.help.llmatlab/LiveLinkForMATLABUsersGuide.pdf (accessed March 4, 2022).

[64] Aboudi J, Arnold SM, Bednarcyk BA. Micromechanics of composite materials: a generalized multiscale analysis approach 2013;1:984.

[65] Chawla KK. Macromechanics of composites. compos mater 1998:347–76. https://doi.org/10.1007/978-1-4757-2966-5_11.

[66] COMSOL AB. Composite materials module. User's Guid 2018:48.

[67] Reissner E. The effect of transverse shear deformation on the bending of elastic plates. J Appl Mech 1945;12:A69–77. https://doi.org/10.1115/1.4009435.

[68] Mindlin RD. Influence of rotatory inertia and shear on flexural motions of isotropic, elastic plates. collect pap Raymond D Mindlin Vol I 1989:225–32. https://doi.org/10.1007/978-1-4613-8865-4_29.

[69] Abrate S, Di Sciuva M. Equivalent single layer theories for composite and sandwich structures: A review. Compos Struct 2017;179:482–94. https://doi.org/10.1016/j.compstruct.2017.07.090.

[70] Industrial additive manufacturing platform | Markforged n.d. https://markforged.com/ (accessed March 23, 2022).

[71] 3DPrint.com - The voice of 3d printing n.d. https://3dprint.com/ (accessed March 23, 2022).

[72] Bárnik F, Vaško M, Handrik M, Dorčiak F, Majko J. Comparing mechanical properties of composites structures on Onyx base with different density and shape of fill. Transp Res Procedia 2019;40:616–22. https://doi.org/10.1016/j.trpro.2019.07.088.

[73] Bárnik F, Vaško M, Ságа M, Handrik M, Sapietová A. Mechanical properties of structures produced by 3D printing from composite materials. MATEC Web Conf 2019;254:01018. https://doi.org/10.1051/matecconf/201925401018.

[74] Composite Base n.d.

[75] Standard test method for tensile properties of polymer matrix composite materials n.d. https://www.astm.org/d3039_d3039m-08.html (accessed March 23, 2022).

[76] ASTM D 7264/D 7264M - 2021 - Beuth.de n.d. https://www.beuth.de/de/norm/astm-d-7264-d-7264m/337538978 (accessed

March 24, 2022).

[77] Matveev MY, Brown LP, Long AC. Efficient meshing technique for textile composites unit cells of arbitrary complexity. Compos Struct 2020;254:112757. https://doi.org/10.1016/J.COMPSTRUCT.2020.112757.